Three zone modeling of Downdraft biomass Gasification: Equilibrium and finite Kinetic Approach

Roshan Budhathoki

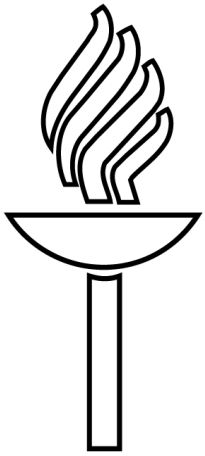

Master's thesis
Master's Degree Program in Renewable Energy
Department of Chemistry, University of Jyväskylä
Supervisor: Professor Jukka Konttinen
March 11, 2013

Abstract

Mathematical models and simulations are being practiced exceedingly in the field of research and development work. Simulations provide a less expensive means of evaluating the benefits and associated risk with applied field. Gasification is a complex mechanism, which incorporates thermochemical conversion of carbon based feedstock. Therefore, simulation of gasification provides a better comprehension of physical and chemical mechanism inside the gasifier than general conjecture and assist in optimizing the yield.

The main objectives of present thesis work involve formulation of separate sub-model for pyrolysis and oxidation zone from published scientific references, and assembling it with provided existing irresolute model of reduction zone to establish a robust mathematical model for downdraft gasifier. The pyrolysis and oxidation zone is modeled with equilibrium approach, while the reduction zone is based on finite kinetic approach. The results from the model are validated qualitatively against the published experimental data for downdraft gasifier. The composition of product gas has been predicted with an accuracy of ~92%. Furthermore, the precision in temperature prediction assists the gasifier designer for proper selection of material, while precision in gas composition prediction helps to optimize the gasification process.

Lower moisture content in the biomass and equivalence ratio lower than 0.45 are proposed as optimal parameters for downdraft gasification of woody biomass. However, the model is found to be incompetent for prediction of the gas composition at higher equivalence ratio. Thus, due to several uncertainties and incompetence of present model at higher equivalence ratio, further need of development of model has been propounded.

Acknowledgements

This master's Thesis was carried out at Department of Chemistry, University of Jyväskylä between 20th October 2012 and 11th March 2013.

I would like to express my deepest gratitude to Prof. Jukka Konttinen for his support and guidance during this thesis and supervising it on the behalf of the University of Jyväskylä.

I would also like to thank Department of Chemistry, University of Jyväskylä and Brazilian CNPq-Project for funding this thesis.

Jyväskylä
March 11, 2013

Roshan Budhathoki

List of Symbols

Upper Case letters		**Units**
A,B,C,D	thermodynamic constants	-
A	activity factor	(1/s)
B	biomass	-
G	Gibbs free energy	(kJ/kmol)
$\overline{G}$	Standard Gibbs free energy	(kJ/kmol)
I,J	thermodynamic constants	(kJ/kmol)
K_{eq}	equilibrium constant	-
M	molecular mass	(kg/kmol)
MC	moisture content (%)	-
N	total number of species	-
P	partial pressure	(Pa)
Q	heat loss	(kJ/kmol)
R	gas constant	(kJ/kmol.K)
R_i	rate of formation of i species	(mol/m^3.s)
S	entropy	(J/K)
T	temperature	(K)

Lower Case letters		**Units**
a	mol of air	(mols)
a_i	number of atom	-
c	mol of carbon in biomass	(mol)
c_p	specific heat capacity	(J/kg.K)
e	exponential	-
g^0	Gibbs function	(kJ/kmol)
h	mol of hydrogen in biomass	(mol)
h_f	heat of formation	(kJ/kmol)
h_{vap}	enthalpy of water vapor	(kJ/kmol)
k	kinetic rate constant	(mol/s)
m	mass	(g/kg)
n	no. of mol	-
$\dot{n}$	rate of formation of species	(mol/s)
o	mol of oxygen in biomass	(mol)
r	rate of reaction	(mol/m^3.s)
t_{res}	residence time	(s)
vol	volatiles	-
w	mol of water	(mol)
y_i	composition fraction	-
v	velocity	(m/s)
z	length of n section in reduction zone	(m)

Greek letters

Δ	change in state
$\sum$	summation of quantities
∂	partial derivative
d	derivative
ρ	density
λ	equivalence ratio

Subscripts

am	arithmetic mean
atm	atmospheric
cl	cellulose
d.b.	dry basis
f	formation
hc	hemicellulose
i	chemical species
j	no. of gasification reaction
lg	lignin
n	section in reduction zone
ox	oxidation zone
p	pyrolysis zone
pt	product
r	reactant
R	reduction zone

Superscripts

0	standard state
E	activation energy
n	section in reduction zone

Mathematical operators

+	addition
-	subtraction
× or '.'	multiplication
/ or —	division

Contents

1 Introduction

Gasification is the thermochemical conversion of solid or liquid feedstock into valuable and convenient gaseous fuel or chemical products which can further be utilized to release thermal energy, power or used in biorefinery applications to produce value added chemicals and liquid biofuels [1]. Direct gasification is considered as an auto-thermal process as it supplies the required thermal energy by partial oxidation or combustion of the supplied feedstock [1, 2].

A typical biomass gasification process usually includes following steps and can be illustrated schematically as in Figure 1.1.

- Drying
- Pyrolysis
- Partial oxidation of pyrolysis product
- Gasification of decomposition product

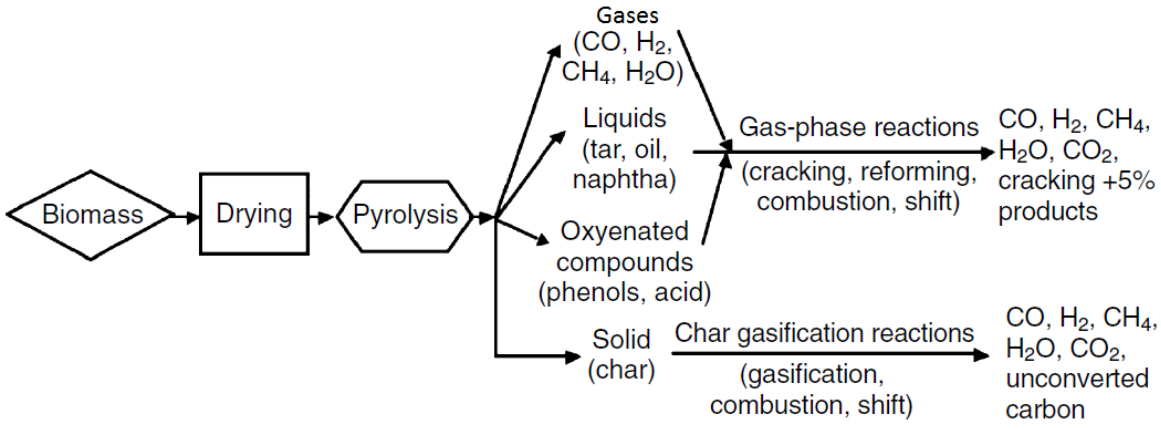

FIGURE 1.1 Schematic paths of gasification process.[1]

During the mathematical simulation of the gasification process, these steps are modeled in series, though there are no sharp boundaries between them and they often overlap [1]. The sequential distinction amongst the steps provides a vivid pathway for mathematical modeling and makes the simulation process simpler and less sophisticated. Furthermore, different gasification technologies presume a particular step sequence to simplify the gasification process.

Gasification reactor designs have been investigated on several aspects, which can be classified as follows:

- *By gasification agent*: The performance of any gasifier is greatly affected by the gasification agent. Currently, air-blown gasifier, oxygen gasifier and steam gasifier have been successfully demonstrated and operated. Use of different gasification agent mainly affects the process parameter like temperature, final composition of the product gas and overall efficiency of the process. Identification of gasification agent provides a great aid in mathematical modeling [1].
- *By heat source*: A gasifier may either be auto-thermal or allothermal in nature. Auto-thermal (direct) gasifiers generate required heat by partial combustion of biomass and allothermal (indirect) gasifiers demand external source of heat via a heat exchanger or indirect process. Heat source assessment provides a clear vision for study of heat transfer and energy balance in simulation [1].
- *By gasifier pressure*: A gasifier may operate in either atmospheric condition or pressurized. During kinetic modeling, characterization of gasifier based on gasifier pressure plays an important role [1].
- *By reactor design*:
- *Fixed-bed gasifier:* The examples of fixed-bed gasifiers are updraft, downdraft, cross-draft and open core. In updraft gasifier (Fig. 1.2(a)), the fuel and the product gases flow in counter direction. During simulation, it follows the sequence of drying, pyrolysis, reduction and oxidation. Moreover, in downdraft gasifier (Fig 1.2(b)), the fuel and the product gases flow in same direction and during simulation, it presumes the step sequence as drying, pyrolysis, partial oxidation and reduction. While cross-flow and open core gasifier may not be modeled in a sequence as, there are no sharp boundaries between the processes. However, simulation can be done even for those processes without any boundaries by either equilibrium modeling or kinetic modeling approach [2].
- *Fluidised-bed gasifier*: Bubbling bed, circulating bed (Fig 1.2(c)) and twin-bed are the common types of fluidized bed gasifier. The gasifying agent is blown from the bed of solid particles at a sufficient velocity in order to keep the particles as well as the bed materials (e.g. sand) in state of suspension. There are no clear system boundaries for the various processes like drying, pyrolysis, oxidation and reduction. In such system, there are a lot of parameters (such as superficial velocity, particle size, gasifier pressure, hydrodynamics and char reactivity) that plays an important role in the performance of the model. Thus, it demands a sophisticated model to predict process conditions. However, several kinetic modeling approaches have been projected with good agreement to the experimental analysis [2].
- *Entrained-flow*: In entrained-flow gasifier (Fig 1.3(d)), ground or slurry fuels especially coal are fed in direct gasification mode and are characterized by short residence time, high temperature, pressure, and

large capacities. These are considered as unsuitable for biomass because of requirement of ground or slurry fuel [2].

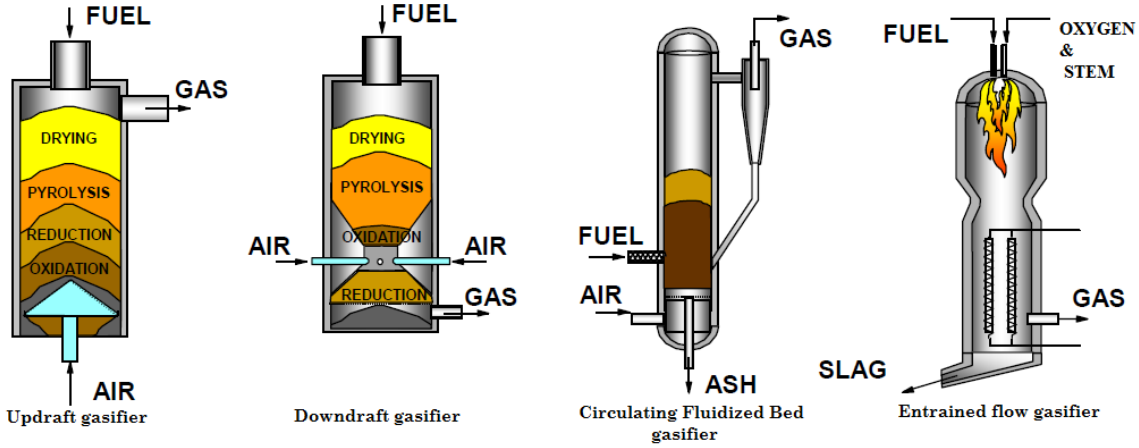

FIGURE 1.2 Schematic of different types of gasifiers.

Figure 1.2 displays the schematic of different commercially operated gasifiers based on the gasifier design. As described earlier, the process sequence of gasification process is determined by the gasifier design. Gasification process in fixed bed gasifier may be divided mainly into pyrolysis, oxidation and reduction sub-zone, whereas there are no clear distinction between these processes in fluidized bed gasifier. For example, downdraft gasifier is proposed to have a sequential order of drying, pyrolysis, partial oxidation and finally reduction. In drying, the biomass feedstock receives enough thermal energy from hot zone downstream to release the water molecule associated with it. The loosely bound water is irreversibly removed above 100^{o}C and low molecular weight extractive start volatilizing, which may last till the temperature reaches up to 200^{o}C. Pyrolysis, in general, involves the thermal breakdown of larger hydrocarbon molecules of biomass into smaller condensable and non-condensable gas molecules at the temperature range of 300 to 1000^{o}C. The important product of pyrolysis is tar, which can create a great deal of difficulty in industrial use of gasification products and exacerbate the accessories units (like gas cleaning system and power generating engines) of the CHP (Combined Heat and Power) plants. Exothermic oxidation/combustion reactions oxidize most of the pyrolysis products and supply the required amount of heat of reaction for endothermic gasification reaction. The typical oxidation temperature during the gasification process is around 1000 to 1300^{o}C. The final step is reduction, which is mainly focused on reforming and shift reactions between the previously formed gas products [1]. In contrast, such order of physical and chemical phenomena is not possible in fluidized bed gasifiers.

2 Objectives of thesis work

The main objective of present thesis work is to amend the existing (provided) kinetic model of reduction zone, which was initially modeled by Pierre E. Conoir, an internship student at University of Jyväskylä in summer 2011. Moreover, the utility of model was limited only to study the influence of moisture content in the feedstock and the model did not incorporate the air to fuel equivalence ratio, which is one of the important parametric properties associated with the gasification process.

In addition, the aim of present work also involves study of different aspects of modeling of downdraft gasification, collect experimental results along with operational parameters and prepare a literature review, expanding the utility of previous model by constructing a revised version of mathematical model for pyrolysis and oxidation zone sub-model from published references, and integrating each of the sub-models. More emphasis is given on formulation of mathematical model that has competence to simulate the complex behavior of downdraft gasification and provide a better comprehension of gasification mechanisms over theoretical conjecture. The objective also includes utilization of thus established model to optimize the gasification parameter for higher benefits.

3 Simulation of Gasification

Mathematical simulation is one of the most important aspects of research and development work such as development of Gasification technology. Though it may not provide a very accurate prediction of system's performance, it may provide qualitative guidance on the effect of design, input variables and operating conditions. Moreover, modeling may provide a less expensive means of evaluating the benefits and the associated risk in the real time scenario [1]. The gasification process depends on number of complex chemical reactions, including fast pyrolysis, partial oxidation, conversion of tar and lower hydrocarbons, water-gas reaction, methane formation reaction. Thus, such complicated process, coupled with the sensitivity of the product distribution to the residence time, their dependence on temperature and pressure as well as rate of heating in the reactor, demands the development of mathematical models to evaluate the process condition [3]. In addition, comprehension of chemical and physical mechanisms of the biomass gasification is essential to optimize the gasifier designing and operating biomass gasification systems [4].

The importance of simulation can be summarized as follows [1]:

- Allows optimizing the operation or design of the plant using available experimental data from a pilot plant or large scale plant.
- Identify the operating limits and associated risks.
- Provide information on extreme operating conditions where experiments and measurements are difficult to perform.
- Assist in interpretation of experimental results and analyze anomalous behavior of the gasifier.
- Aid in the scale-up of the gasifier from one successfully operating size to another and from one feedstock to another.

Gasifier simulation models may be classified into thermodynamic equilibrium model, kinetic model, computational fluid dynamics (CFD) model and artificial neural network. All these models approach different methods to assess the prediction of the one's model and have different utility and limitations. However, modeling of a gasification using different approach may consider following reaction as basic gasification reaction [5, 6]:

Boudouard reaction (R1): $C + CO_2 \rightarrow 2CO$ (3.01)

Water-gas reaction (R2): $C + H_2O \rightarrow H_2 + CO$ (3.02)

Methane formation (R3): $C + 2H_2 \rightarrow CH_4$ (3.03)

Steam reforming reaction (R4): $CH_4 + H_2O \rightarrow H_2 + CO_2$ (3.04)

3.1 Thermodynamic Equilibrium Model [7]

Thermodynamic equilibrium models are based on the chemical and thermodynamic equilibrium, which is determined by implication of equilibrium constants and minimization of Gibbs free energy. At chemical equilibrium, the system is considered to be at its most stable composition, which means the entropy of system is maximized, while its Gibbs free energy is minimized. Though chemical or thermodynamic equilibrium may not be reached within the gasifier, equilibrium models provide a designer with reasonable prediction for the final composition and monitor the process parameter like temperature [5]. Some major assumptions of thermodynamic equilibrium can be presented as:

- The reactor is considered as zero dimensional [8].
- There is perfect mixing of materials and uniform temperature in the gasifier although different hydrodynamics are observed in practice [5].
- The reaction rates are fast enough and residence time is long enough to reach the equilibrium state [9].

Equilibrium models are independent of gasifier design and cannot predict the influence of hydrodynamics or geometric parameters like fluidizing velocity, design variables (gasifier height). However, these models are quite convenient to study the influence of fuel and the process parameter and can predict the temperature of the system [3]. Thermodynamic equilibrium models can be approached by either stoichiometric or nonstoichiometric methods.

3.1.1 Stoichiometric Equilibrium Models [3]

Stoichiometric equilibrium models incorporate the thermodynamic and chemical equilibrium of chemical reactions and the species involved. The model can be designed either for a global gasification reaction or can be divided into sub-model for drying, pyrolysis, oxidation and reduction.

3.1.1.1 Single step stoichiometric equilibrium model [7]

This model embodies the several complex reaction of gasification into one generic reaction as mentioned in Eq. (3.05). It assumes that one mole of biomass CH_hO_o, based on a single atom of carbon that is being gasified with w mol of water/steam in presence of a mole of air [7].

$$CH_hO_o + wH_2O + a(O_2 + 3.76N_2) = n_C C + n_{H_2} H_2 + n_{co} CO + n_{co_2} CO_2 + n_{CH_4} CH_4 + n_{H_2O} H_2O + 3.76a\, N_2 \quad (3.05)$$

In the above equation, *w* and *a* are the variables and changed in order to get desired amount of product. There are six unknowns are $n_C, n_{H_2}, n_{co}, n_{co_2}$, n_{CH_4} and n_{H_2O}. Based on stoichiometric balance of carbon, hydrogen and oxygen, following equations are obtained:

Carbon balance: $$n_C + n_{co} + n_{co_2} + n_{CH_4} = 1 \quad (3.06)$$

Hydrogen balance: $$2n_{H_2} + 4n_{CH_4} + 2n_{H_2O} = 2w + h \quad (3.07)$$

Oxygen balance: $$n_{co} + 2n_{co_2} + n_{H_2O} = w + 2a \quad (3.08)$$

As Boudouard reaction, water-gas reaction, methane formation and steam reforming reaction are considered as the major reaction of gasification, the equilibrium constants (K_{eq}) for reactions R1, R2, R3 and R4 are given as [10]:

$$K_{eq,1} = \frac{n_{CO}^2}{n_{CO_2}} \quad (3.09)$$

$$K_{eq,2} = \frac{n_{H_2}.n_{CO}}{n_{H_2O}} \quad (3.10)$$

$$K_{eq,3} = \frac{n_{CH_4}}{n_{H_2}^2} \quad (3.11)$$

$$K_{eq,4} = \frac{n_{H_2}.n_{CO_2}}{n_{CO}.n_{H_2O}} \quad (3.12)$$

The combination of Eq. (2.05) to Eq. (2.11) results in sophisticated polynomial equations that can be solved by multiple and simultaneous iteration using advance mathematical programs and it may requires plentiful assumptions.

If the gasification process is assumed to be adiabatic, then the energy balance of the gasification reaction results to a new set of equation, which can determine the final temperature of the system [7, 11].

$$\sum_i n_i \left[h_{f,i}^0 + \Delta H_{298}^T\right]_{i,Reactant} = \sum_i n_i \left[h_{f,i}^0 + \Delta H_{298}^T\right]_{i,Product_{loss}} \quad (3.13)$$

Modifying Eq. (3.13) on the basis of Eq. (3.05), we get:

$$h^0_{f,wood} + w(h^0_{f,H_2O(l)} + h_{vap}) + ah^0_{f,O_2} + 3.76ah^0_{f,N_2} = n_C.h^0_{f,C} + n_{H_2}h^0_{f,H_2} + n_{co}h^0_{f,CO} + n_{co_2}h^0_{f,CO_2} + n_{CH_4}h^0_{f,CH_4} + n_{H_2O}h^0_{f,H_2O} + 3.76a\,h^0_{f,N_2} + \Delta T(n_C c_{p,C} + n_{H_2}c_{p,H_2} + n_{co}c_{p,CO} + n_{co_2}c_{p,CO_2} + n_{CH_4}c_{p,CH_4} + n_{H_2O}c_{p,H_2O} + 3.76ac_{p,N_2})$$

(3.14)

where h^0_f for biomass(wood) can be estimated by the application of Hess law, as described in Appendix A1. In this equation, $h^0_f, c_{p,C}, h_{vap}$ represents heat of formation of corresponding chemical species, specific heat capacity and enthalpy of vaporization of water respectively and $\Delta T = T_{gasification} - T_{ambient}$ refers to temperature difference between the gasification temperature and the ambient or the initial temperature of biomass feedstock [1, 7]. The heats of formations for different chemical compounds are given in the Appendix B1 and the specific heat of corresponding compounds can be estimated by using different correlations.

Thus, single step stoichiometric equilibrium model may be formulated by the application of the chemical equilibrium state and the reaction stoichiometric condition.

3.1.1.2 Sub-models for stoichiometric equilibrium model [12]

This model incorporates modeling of separate sub-model for drying, pyrolysis, oxidation and reduction. The output from one sub-model becomes input for the successive sub-model. This model has more utility than the single step stoichiometric equilibrium model as the composition and temperature at different zone can be assessed with the aid of sub-model. Several combinations (as illustrated in Figure 2.1) of sub-models can be achieved and can be selected as per the requirement of the model and its feasibility.

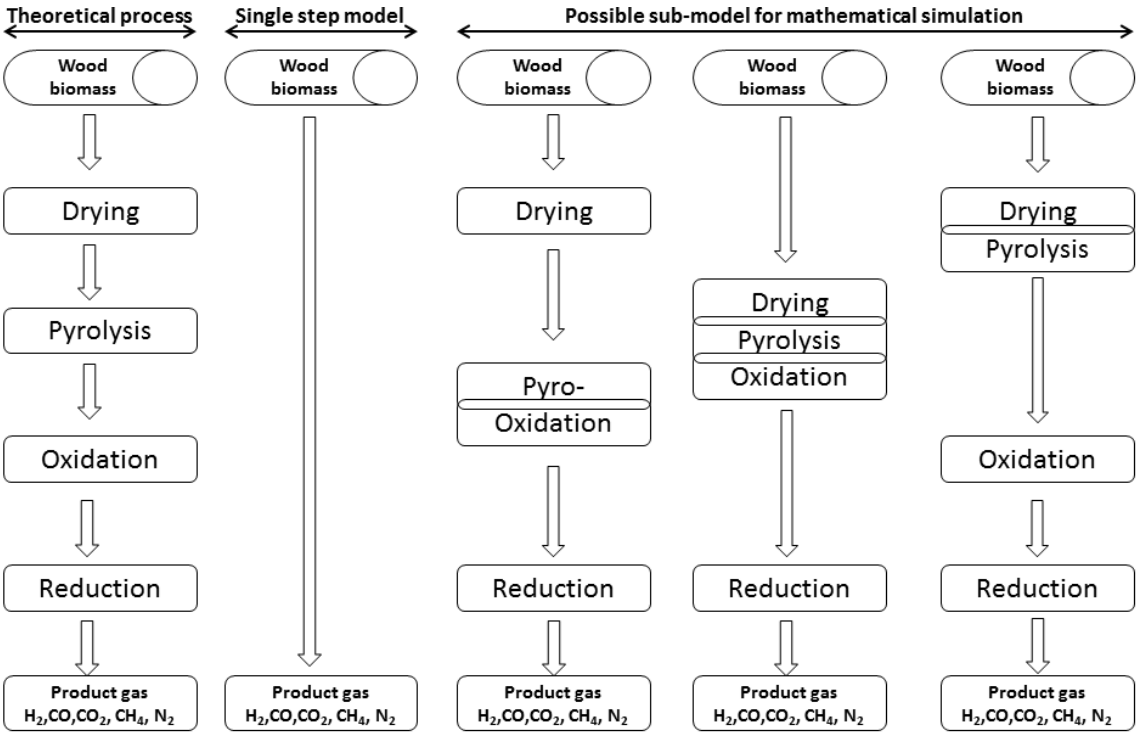

Figure 3.1 Possible sub-models for conversion of biomass to product gas

For the sake of convenience and clarity of sub-model, sub-models for drying and pyrolysis, oxidation and reduction zone have been proposed for the current paper. However, the modeling approach follows similar principle as that of single step stoichiometric equilibrium model regarding the mathematical formulation. One of the uncertainties of such sub-model lies in their assumption for final product. For example, the assumptions implied in pyrolysis sub-model indicate that that the product composition mainly includes CO, CO_2, H_2, H_2O, CH_4 and tar with higher concentration of lighter component as in Eq. (3.14) [13]. The compositions of pyrolysis products are dependent to heating rate and the pyrolysis temperature, thus such assumptions may not be valid practically, but provide a great aid on overall modeling of the gasification process. Then, the pyrolysis products are subjected as input for the next sub-model. In case of downdraft gasifier, it is subjected to oxidation sub-model. The pyrolysis products undergo partial oxidation in presence of non-stoichiometric oxygen supply, and the reaction in oxidation sub-model may be proposed as in Eq. (3.15) [12, 14]. The course of reaction during oxidation is also quite uncertain; however such generic reaction provides simplicity during simulation process. Finally, the products from the oxidation zone are subjected for reduction sub-model as input. The reduction sub-model employ char and shift reactions as mentioned in Eq. (3.01-3.04) and the overall generic reaction may be modeled as in Eq. (3.16) [12].

Modeled reaction for pyrolysis sub-model*:*

$$CH_hO_o + wH_2O \rightarrow n_{p,C}C + n_{p,CO_2}CO_2 + n_{p,CO}CO + n_{p,CH_4}CH_4 + n_{p,H_2}H_2 + n_{p,C_2H_2}C_2H_2 + n_{p,H_2O}H_2O \quad (3.15)$$

Modeled reaction for oxidation sub-model:

$$n_{p,C}C + n_{p,CO_2}CO_2 + n_{p,CO}CO + n_{p,CH_4}CH_4 + n_{p,H_2}H_2 + n_{p,C_2H_2}C_2H_2 + n_{p,H_2O}H_2O + a(O_2 + 3.76N_2) \rightarrow n_{ox,C}C + n_{ox,CO_2}CO_2 + n_{ox,CO}CO + n_{ox,CH_4}CH_4 + n_{ox,H_2O}H_2O + 3.76aN_2 \quad (3.16)$$

Modeled reaction for reduction sub-model:

$$n_{ox,C}C + n_{ox,CO_2}CO_2 + n_{ox,CO}CO + n_{ox,CH_4}CH_4 + n_{ox,H_2O}H_2O + 3.76aN_2 = n_{R,C}C + n_{R,CO_2}CO_2 + n_{R,CO}CO + n_{R,H_2}H_2 + n_{R,CH_4}CH_4 + n_{R,H_2O}H_2O + 3.76aN_2 \quad (3.17)$$

Generic energy balance model:

$$\sum_i n_i \left[h^0_{f,i} + \Delta H^T_{298}\right]_{i,Reactant} = \sum_i n_i \left[h^0_{f,i} + \Delta H^T_{298}\right]_{i,Product} + Q_{loss} \quad (3.18)$$

The solution of Eq. (3.14-3.18) involves similar computational approach by employing chemical equilibrium state and stoichiometric condition as mentioned in section 3.1.1.1. Moreover, the computation can also be approached with several empirical approximations as mentioned in [12].

3.1.2 Non-stoichiometric Equilibrium Model [8]

The non-stoichiometric equilibrium model is solely based on minimizing Gibbs free energy of the system and there is not any specification for particular reaction mechanisms. However, moisture content and elemental composition of the feed is needed which can be obtained from the ultimate analysis data of feed. Therefore, this method is particularly suitable for fuels like biomass whose exact chemical formula is not distinctly known [1, 3].

The Gibbs free energy, G_{total} for the gasification product which consists of N species (i= 1…N) is represented as in Eq. (3.19) [11].

$$G_{total} = \sum_{i=1}^{N} n_i \Delta G^0_{f,i} + \sum_{i=1}^{N} n_i RT \ln\left(\frac{n_i}{\sum n_i}\right) \quad (3.19)$$

where $\Delta G^{0}_{f,i}$ is the standard Gibbs energy of i species, R is gas constant. The solution of Eq. (3.19) for unknown values of n_i is approached to minimize G_{total} of the overall reaction considering the overall mass balance. Though, non-stoichiometric equilibrium model does not specify the reaction path, type or chemical formula of the fuel, the amount of total carbon obtained from the ultimate analysis must be equal to sum of total of all carbon distributed among the gas mixtures (Eq.(3.20)) [8].

$$\sum_{i=1}^{N} a_{i,j} n_i = A_j \tag{3.20}$$

where a_i is the number of atoms of the j element and A_j is the total number of atoms of j^{th} element in reaction mixture. The objective of this approach is to find the values of n_i such that the G_{total} will be minimum. Lagrange multiplier method is the most convenient and proximate way to solve these equations [15]. Thus, the Lagrange function (L) can be defined as

$$L = G_{total} - \sum_{j=1}^{K} \lambda_j \left(\sum_{i=1}^{N} a_{ij} n_i - A_i \right) \tag{3.21}$$

where λ is Lagrangian multipliers. The equilibrium is achieved when the partial derivatives of Lagrange function are zero. i.e.,

$$\left(\frac{\partial L}{\partial n_i} \right) = 0 \tag{3.22}$$

Dividing Eq. (3.21) by RT and substituting the value of G_{total} from Eq. (3.19), then taking its partial derivate results to Eq. (3.23) [16].

$$\left(\frac{\partial L}{\partial n_i} \right) = \frac{\Delta G^{0}_{f,i}}{RT} + \sum_{i=1}^{N} \ln \left(\frac{n_i}{n_{total}} \right) + \frac{1}{RT} \sum_{j=1}^{K} \lambda_j \left(\sum_{i=1}^{N} a_{ij} n_i \right) = 0 \tag{3.23}$$

The standard Gibbs free energy of each chemical species can be obtained by subtracting the standard enthalpy from the standard entropy multiplied by a specific temperature of the system as in Eq. (3.24) [1, 16].

$$\Delta \bar{G}^{0}_{j,i} = \Delta \bar{H}^{0}_{f,i} + T \Delta \bar{S}^{0}_{f,i} \tag{3.24}$$

where $\Delta \bar{S}^{0}_{f,i}$ is the standard entropy of i species. According to first law of thermodynamics, the energy balance of the non-stoichiometric equilibrium model can be achieved by Eq. (3.25) [1, 17].

$$\sum_{r=reactant} n_r \overline{H}_r^0(T_r) + Q_{loss} = \sum_{pt=product} n_p \overline{H}_{pt}^0(T_{pt}) + \Delta H \quad (3.25)$$

Thus, the final compositions of the product gas can be determined via non-stoichiometric equilibrium approach. Moreover, this model gives the utility to examine the effect on product gas composition and temperature by changing the moisture content and biomass feed. However, such models have plenty of limitations.

Table 3.1 displays a short review on different aspects of thermodynamic equilibrium model for fixed bed downdraft gasifier based on the computational approach, results and validations. Most of the equilibrium models are subjected to study the influence of moisture content. Ratnadhariya et al. [12] proposed separate sub-model for different steps of downdraft gasification process and employed the model to investigate the effect of equivalence ratio on product gas composition and the temperature profile. The prediction of model was not supportive for higher equivalence ratio when compared to the test results.

Table 3.1 Review analysis of thermodynamic equilibrium model for fixed bed downdraft gasifier

Ref.	Authors	Equilibrium model	Modeling approach	Computational Method/Tool	Results and validations
[7]	Zainal et al. (2001)	Single step stoichiometric equilibrium	~generic reaction is modeled as in Eq. (3.05) ~equation obtained from elemental balance at equilibrium state and from chemical equilibrium expression as in Eq. (3.09-3.12) are non-linear & solved iteratively ~temperature is determined using energy balance relation	Newton-Raphson method	~modeled for CO, CO_2, H_2,CH_4 & N_2 prediction ~supportive validation
[11]	Koroneous et al. (2011)			Trial and error method	~results compared for CO, CO_2, H_2, & CH_4 ~high uncertainty in CO and CH_4 prediction
[12]	Ratnadhariya et al. (2009)	Sub-models for stoichiometric equilibrium	~generic reaction for each zone (pyrolysis, oxidation & reduction) is modeled as in Eq. (3.15-3.17) ~computational approach similar to single step stoichiometric equilibrium modeling	Turbo C++	~validated for CO, CO_2, H_2,CH_4 & N_2 ~good predictability ~uncertainties in CH_4 prediction
[17]	Dutta et al. (2008)	Non-stoichiometric equilibrium	~specific reaction path is not required ~gas composition is determined at minimum Gibbs energy state where equilibrium is supposed to be achieved	Newton-Raphson method	~experimental data of CO,H_2 & CO_2 are compared ~poor predictability ~high uncertainty of CH_4 prediction
[16]	Antonopoulos et al. (2012)			Engineering equation solver (EES)	

Note: Equilibrium model have high uncertainty in CH_4 prediction as the methane formation reaction does not attain the equilibrium state at normal gasification temperature [7].

3.2 Kinetic Model [18]

The inadequacy of equilibrium model to conjoint the reactor design parameter with the final composition of product gas or the outcome of the model reveals the need of kinetic models to evaluate and imitate the gasifier behavior. A kinetic model allows predicting the gas yield, product composition after finite residence time in finite volume and temperature inside the gasifier. Moreover, it involves parameter such as reaction rate, residence time, reactor hydrodynamics (superficial velocity, diffusion rate) and length of reactor [1]. Thus, kinetic model provides a wide dimension to investigate the behavior of a gasifier via simulation and they are more accurate but computationally intensive [3].

As biomass gasification is quite an extensive process that it is difficult to formulate the exact reaction pathways and difficult to simulate. Numerous researches have been conducted on kinetic modeling of biomass gasification. Most of models accounts for modeling for reduction reaction and often separate sub-model for pyrolysis, oxidation and reduction. Separating the overall process into sub-model of pyrolysis, oxidation and reduction zone help in simplifying the model and provide better understanding of the downdraft gasifier behavior.

3.2.1 Sub-model of pyrolysis zone [19]

Pyrolysis is a complex mechanism and can be described as the function of heating rate and residence time. The decomposition products of pyrolysis vary greatly depending upon biomass selection, heating rate and residence time as well [19]. Thus, a vivid reaction scheme is hard to establish and is not universal. In addition, it is also difficult of obtain reliable data of kinetic constants which is universal and can be implicated in general. Due to the difficulty in the determination of kinetic parameter for fast pyrolysis, biomass pyrolysis during gasification can be considered as slow rate, since some reasonable value of kinetic parameters can be obtained [20]. It has been observed that the kinetic models for pyrolysis are established based on the composition of the cellulose, hemicellulose and lignin rather than the ultimate analysis as that of the equilibrium models.

Kinetic models of pyrolysis may be described based on one-stage global single reaction, one-stage multiple reactions and two-stage semi global reaction. This paper focuses only on one-stage global single reaction, which may be represented as:

$$C_cH_hO_o = n_{Char}C + n_{CO_2}CO_2 + n_{CO}CO + n_{CH_4}CH_4 + n_{H_2}H_2 + n_{H_2O}H_2O + n_{tar}C_{tc}H_{th}O_{to} \quad (3.26)$$

Several kinetic models for pyrolysis have been proposed based on several reaction schemes as described in [21]. One simple approach for modeling fast pyrolysis has been demonstrated by A.K. Sharma [22]. For the simplicity of the model, following assumptions can be invoked [22]:

- Char yield in the gasifier is independent to pyrolysis temperatures encountered in pyrolysis zone.
- The volatiles are composed of mainly H_2, CO, CO_2, H_2O and tar.

The actual rate of pyrolysis depends on the unpyrolyzed mass of biomass or the mass of the volatiles in the biomass [20, 22]. Thus, the rate of devolatization may be expressed as

$$\frac{dm_{vol}}{dt} = -km_{vol} \tag{3.27}$$

where m_{vol} is the mass of volatiles. If the kinetic rate constant is expressed in terms of Arrhenius equation ($k = A.e^{(-E/RT)}$), then Eq. (3.25) becomes

$$\frac{dm_{vol}}{dt} = A.e^{(E/T)} m_B y_{vol} \tag{3.28}$$

where m_B is mass of biomass, y is the molar fraction of corresponding chemical species and A, E are kinetic parameters. Finally, the change in composition of each volatile may be determined based on following equations [21];

$$\Delta \dot{m}_{vol,i} = \left(\frac{d\dot{m}_{vol}}{dt}\right)_i = \Delta t_{res,i}\left(\frac{dm_{vol}}{dt}\right)_i = \Delta t_{res,i}\left(A.e^{(E/RT)} m_B y_{vol}\right)_i \tag{3.29}$$

where Δt_{res} is the residence time. Similarly, the empirical mass relation as described by Sharma AK may be expressed as [23]:

$$\frac{y_{CO}}{y_{CO_2}} = e^{\left(-1.845 + \frac{7730.3}{T} - \frac{5019898}{T^2}\right)} \tag{3.30}$$

$$\frac{y_{H_2O}}{y_{CO_2}} = 1 \tag{3.31}$$

$$\frac{y_{CH_4}}{y_{CO_2}} = 5 \times 10^{-16} T^{5.06} \tag{3.32}$$

At last, the heat of pyrolysis may be computed with the following expression [19, 23]:

$$\Delta h_p^0 = \left(-h_f^0\right)_{DB} + y_{char}\left(h_f^0\right)_{char} + y_{vol}\sum_{i=1}^{6} y_i \left(h_f^0\right)_i \qquad (3.33)$$

Thus, the iterative solution of Eq. (3.27-3.33) results in the prediction of composition of pyrolysis product, pyrolysis residence time and temperature. These values can be used as initial input for successive oxidation zone [23].

3.2.2 Sub-model of oxidation zone [22]

Oxidation of pyrolysis product in a downdraft gasifier takes place in non-stoichiometric supply of oxygen. Due to variation in reaction time scales and different reactivity of pyrolysis products, some of the reactions might not attain equilibrium in oxidation zone. Thus, scheming of reaction in oxidation zone is very challenging and the kinetic model solely depends on the numbers of reactions proposed for the time being. Sharma A.K. formulated the kinetic model for the reaction occurring in oxidation zone with an assumption that the pyrolysis products like char, CO, H2, other hydrocarbon and biomass itself reacts with non-stoichiometric amount of oxygen. The corresponding kinetic model proposed by Sharma A.K. is formulated in table 3.2.

Table 3.2 Chemical reactions in oxidation zone [22]

Oxidation reactions	Rate expression	Aj	Ej/R
$H_2+0.5O_2 \rightarrow H_2O$	$k_{H_2} = A_{CO} T^{1.5} e^{(-E_{CO}/RT)} [C_{CO_2}][C_{H_2}]^{1.5}$	$1.63E^9$	3420
$CO+0.5H_2 \rightarrow CO_2$	$k_{CO} = A_{CO} e^{(-E_{CO}/RT)} [C_{CO}][C_{O_2}]^{0.25}[C_{H_2O}]^{0.5}$	$1.3E^8$	15106
[a] $C_{1.16}H_4+1.5O_2 \rightarrow 1.16CO+2H_2O$	$k_{ME} = A_{CH_4} e^{(-E_{CH_4}/RT)} [C_{O_2}]^{0.8}[C_{CH_4}]^{0.7}$	$1.58E^9$	24157
[b] $C_6H_{6.2}O_{0.2}+4.45O_2 \rightarrow 6CO+3.1H_2O$	$k_{tar} \cong k_{HC} = A_{tar} T P_A^{0.3} e^{(-E_{tar}/RT)} [C_{O_2}]^1 [C_{HC}]^{0.5}$	$2.07E^4$	41646
$C+0.5O_2 \rightarrow CO$	$k_{char} = A_{char} e^{(-E_{char}/RT)} [C_{O_2}]$	0.554	10824

[a] $C_{1.16}H_4$ (light hydrocarbon or methane-equivalent)
[b] $C_6H_{6.2}O_{0.2}$ (heavy hydrocarbon or tar equivalent)

Whereas, the kinetic model proposed by E. Ranzi et al. [24] describes the kinetic model only for reaction between char and oxygen, and is shown in table 3.3.

Table 3.3 Char combustion reactions in oxidation zone [24]

Oxidation reactions	Rate expression
$Char+O_2 \rightarrow CO_2$	$k = 5.7 \times 10^9 \exp(-38{,}200/RT)[O_2]^{0.78}$
$Char+0.5O_2 \rightarrow CO$	$k = 5.7 \times 10^{11} \exp(-55{,}000/RT)[O_2]^{0.78}$

Thus, there is no universal approach for kinetic modeling of the oxidation reaction or any other reaction. So, one can apply heuristic approach to simulate the oxidation mechanism which is convenient for the whole modeling picture.

3.2.3 Sub-model of reduction zone [25]

The last step of downdraft gasification process is reduction of precedent chemical species from oxidation zone, which comprises the shift and reformation reactions. The mathematical model of reduction zone encompasses some major reactions such as Boudouard reaction, water gas reaction, methane formation reaction, steam reforming reaction and water gas shift reaction as mentioned in Eq. (3.01-3.04). Although, Wang et al. [26] and Giltrap [25] excluded water gas shift reaction from their model as it had a little effect on the global gasification modeling.

The reaction rates (r_i) are considered to have Arrhenius type temperature dependence and the rate of reaction for Eq. (3.01-3.04) can be expressed as [25]:

$$r_1 = A_1 \exp^{\left(\frac{-E_1}{RT}\right)} \cdot \left(P_{CO_2} - \frac{P_{CO}^2}{k_1} \right) \tag{3.34}$$

$$r_2 = A_2 \exp^{\left(\frac{-E_2}{RT}\right)} \cdot \left(P_{H_2O} - \frac{P_{CO} . P_{H_2}}{k_2} \right) \tag{3.35}$$

$$r_3 = A_3 \exp^{\left(\frac{-E_3}{RT}\right)} \cdot \left(P_{H_2}^2 - \frac{P_{CH_4}}{k_3} \right) \tag{3.36}$$

$$r_4 = A_4 \exp^{\left(\frac{-E_4}{RT}\right)} \cdot \left(P_{CH_4} . P_{H_2O} - \frac{P_{CO} . P_{H_2}^3}{k_4} \right) \tag{3.37}$$

where P is the partial pressure of corresponding gaseous species. Once the rates of gasification reactions are determined, the rate of formation of different gaseous species can be expressed in terms of rate of gasification reactions,

which are summarized in table 3.4. R_x indicates to the rate of formation or destruction of species involved in gasification reaction.

Table 3.4 Net rate of formation of gaseous species by gasification reaction [25]

Species	R_x (mol.m^{-3}.s^{-1})
H_2	r_2-2r_3+3r_4
CO	2r_1+r_2+r_4
CO_2	-r_1
CH_4	r_3-r_4
H_2O	-r_2-r_4
N_2	0

The creation and destruction of any species in finite kinetic rate model for reduction zone is generally dependent on several factors such as length, temperature and even flow. The reduction zone is partitioned into z number of compartment with equal length Δz [25]. The products from oxidation zone are taken as initial input for the first compartment of reduction zone. Then, the net creation or destruction of any species on next compartment may be estimated as a function of gas velocity and rate of formation of corresponding species as expressed in Eq. (3.38-3.39) [25, 27].

$$\frac{dn_i}{dz} = \frac{1}{v}\left(R_x - n_i \frac{dv}{dz}\right) \tag{3.38}$$

Modifying Eq. (3.38) and using the boundary condition, we get;

$$n_i^n = n_i^{n-1} + \left[\frac{1}{v_{n-1}}\left(R_x^{n-1} - n_i^{n-1}\frac{v_n - v_{n-1}}{\Delta z}\right)\right] \times \Delta z \tag{3.39}$$

On the other hand, the net creation of species may be determined as a function of compartment volume and rate of formation of species as expressed in Eq. (3.40) [28].

$$n_i^n = n_i^{n-1} + R_x^n \Delta V^n \tag{3.40}$$

where V is the volume of controlled system or z compartment. Several other parameters such as dependency of temperature, pressure, and gas flow may be incorporated with this model and extend the boundary of such model.

Finally, the composition of i species at n^{th} location/compartment is determined by employing Eq. (3.39 or 3.40).

A short review has been done based on the model proposed by several researchers. For example, kinetic model proposed by Sharma (2011) [22] consists of separate sub-model for each zone. Likewise, N. Gao and A. Li [4] prepared a model which consider pyrolysis and reduction zone. Giltrap et al. [25], Babu and Sheth [27], Datta et al. [28] and F. Centeno et al. [14] have even combined equilibrium model and kinetic model together to establish an intensive and robust model. A summary of review on kinetic modeling of downdraft biomass gasification is listed in table 3.5.

Table 3.5 Review analysis of kinetic modeling of downdraft biomass gasification

Ref	Authors	Kinetic model			Operational parametric	Results & Utility
		Pyrolysis sub-	**Oxidation sub-**	**Reduction sub-**		
[25]	Giltrap et al. (2003)	~empirical assumption for devolatilization by the energy released from combustion		~reduction reaction are considered as governing reaction ~focused on char reaction ~Eq.(3.01-3.04) are major modeled reaction ~Eq.(3.39) is employed to estimate the concentration at n^{th} compartment	~moisture content ~C_{RF} ~gas flow ~pressure ~length of reduction zone	~reasonable prediction ~over prediction of methane ~utility not stated
[27]	Babu & Sheth (2005)					
[4]	Li & Gao (2008)	~pyrolysis is modeled at fast heating rate ~ volatiles & char are estimated based on Koufopanos mechanism ~kinetic rates of pyrolysis are accounted based on volatiles	~oxidation is considered but not modeled			~methane over prediction ~effect of residence time and bed length was studied
[22]	Sharma A.K (2011)	~pyrolysis is modeled at slow heating rate ~kinetics of pyrolysis are accounted based on char conversion	~oxidation is modeled based on char and volatiles oxidation as described in table 3.2	~char reaction is principle reaction ~Eq.(3.01-3.04) are major modeled reaction ~Eq.(3.40) is utilized to determine the concentration at n^{th} compartment	~moisture content, C_{RF}, gas flow, pressure, length of reduction zone ~equivalence ratio or air flow ~diffusion rate ~thermal conductivity ~finite fluid flow rate	~good agreement on measured and predicted data ~influence of gas flow rate and temperature were investigated

3.3 Computational fluid dynamics (CFD) Model [29]

Computational fluid dynamics play an important role in modeling of both fluidized-bed gasifier and fixed downdraft gasifier. A CFD model implicates a solution of conservation of mass, momentum of species, energy flow, hydro-dynamics and turbulence over a defined region. Solutions of such sophisticated approach can be achieved with commercial software such as ANSYS, ASPEN, Fluent, Phoenics and CFD2000 [1, 3]. CFD appears to be a cost –effective options to explore the various configurations and operating conditions at any scale to identify the optimal configuration depending on the project specification [29].

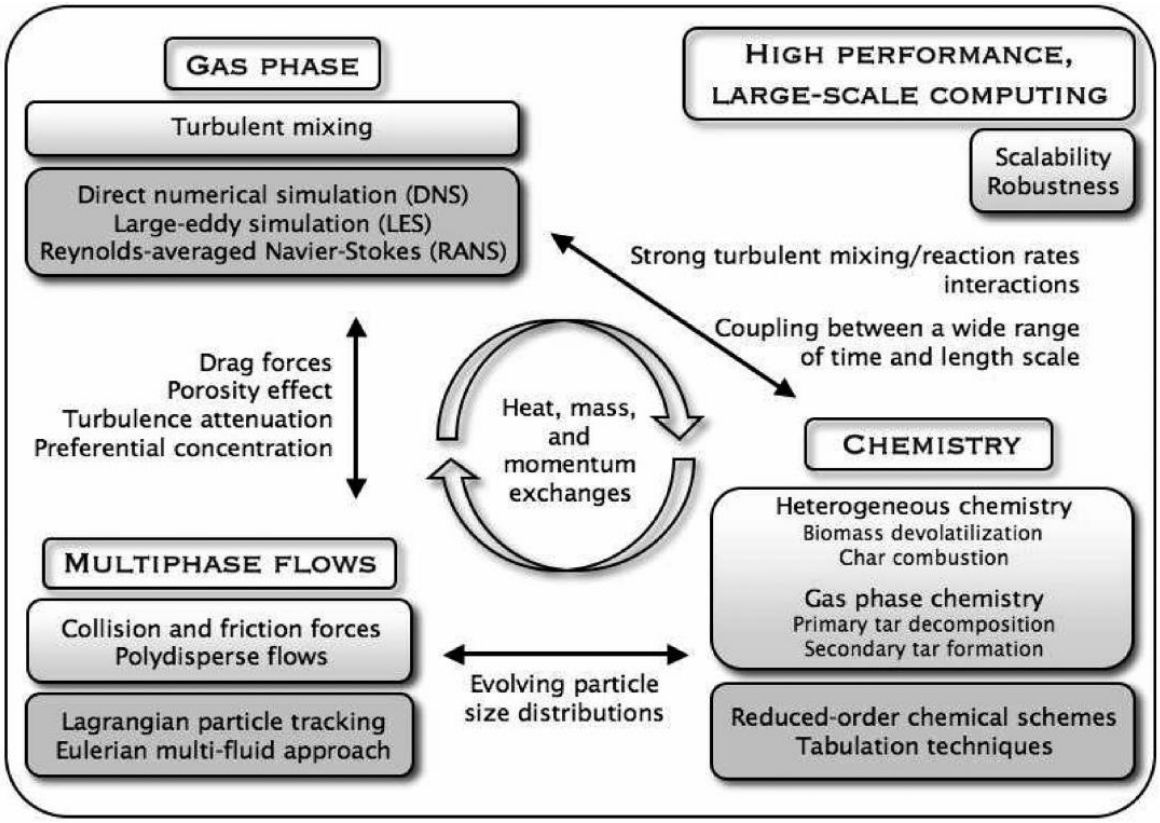

Figure 3.2 Modeling scheme of biomass gasification by CFD approach[29]

Figure 3.2 exposes the several sub-models that are incorporated within the CFD model. CFD modeling involves advanced numerical methods for accounting solid phase description, gas phase coupling and also focuses on the mixing of the solid and gas phase. The turbulent mixing may be modeled by the application of several equations such as Direct Numerical Simulation (DNS), Large-eddy simulation (LES) and Reynolds-averaged Navier-Stokes (RANS) equations Furthermore, complex parametric such as drag force, porosity of the

biomass and turbulence attenuation are mostly taken into consideration. The flow phase is modeled either using Two-fluid model or Discrete particle model. Moreover, the heterogeneous chemistry of biomass gasification including devolatilization, char combustion and gas phase chemistry are modeled simultaneously considering the heat, mass and momentum change at each phase [29, 30].

Comprehensive CFD simulations for biomass gasification are scarce, mainly due to lack of broad computational resources and anisotropic nature of biomass [29]. However, some simplified CFD models had been established to simulate the gasification behavior by Fletcher et al (2000) [31], Yu et al. (2007) [32] and Janajreh et al. (2013) [30]. These CFD models are reviewed and several characteristics related with CFD models are summarized shortly in Table 3.5. The summarized characteristics include the type of gasifier being simulated, fuel used for gasification, dimension of model, particle and phase model, chemistry involved in gasification and finally its validation. The CFD models reveal promising results that indeed are beneficial for further investigation on hydrodynamic inside the gasifier. However, modeling of tar is quite challenging even in CFD modeling [29, 30].

Table 3.5 Review of CFD modeling for gasification

Authors	Fletcher et al (2000).	Yu et al. (2007)	Janajreh et al.(2013)
Ref	[31]	[32]	[30]
Fuel	Biomass	Coal	Biomass
Application	Gasification in entrained/downdraft flow gasifier	Gasification in fluidized bed	Gasification in downdraft gasifier
Dimensions	3	2	2
Model	Discrete particle model (DPM)	Two-fluid model (TFM)	Discrete particle model (DPM)
Multiphase	Lagrangian	Eulerian	Lagrangian
Turbulence	Reynolds-averaged Navier-Stocks (RANS)	RANS	RANS
Chemistry	Multi-step reactions for CO,CO2, H2O, H2, CH4 and Char	Multi-step reactions for CO,CO2, H2O, H2, CH4 and Char	Multi-step reactions for CO,CO2, H2O, H2, CH4 and Char
Validation with experiments	Very limited (exit gas composition)	Major species of product gas (CO,H2, CO2)	None

3.4 Artificial neural networks (ANNs) Model [1]

Artificial neural networks (ANNs) modeling may be considered as a computational paradigm in which a dense distribution of simple processing element is supplied to provide a representation of complex process including nonlinear and discrete systems. ANNs is a standard modeling tool consisting of multilayer perceptron (MLP) paradigm [33]. MLP further consists of an input, a hidden and an output layer of neurons [1, 33]. A schematic of a multilayer neural network is presented in Figure 2.9.

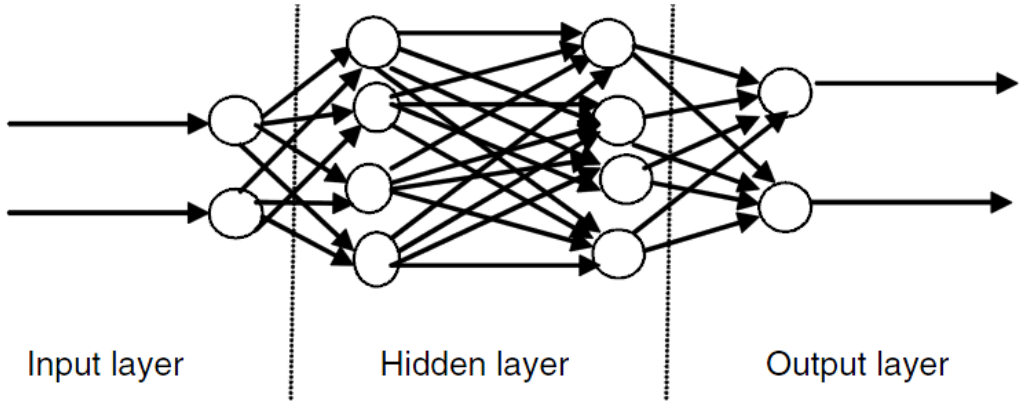

Figure 2.9 Schematic of a multilayer feed-forward neural network [1].

The neurons in the input layer consisting inputs and weights, simply forward the signals to the hidden neurons. While, each neuron in the hidden and output layer has a threshold parameter known as bias. ANNs models are mostly characterized as non-mechanistic, non-equilibrium and non-analytical model [1, 3]. However, it can produce numerical results that can be used to predict the composition of product gas from the gasifier.

The neural network simulation of downdraft gasifier requires an extensive set of data-base, which consists of large amount of experimental downdraft biomass gasification data. Thus, collected data is used as input in artificial neural network modeling. The next step involves the training of the network and its validation that can be successfully achieved with the help of Statistical Neural Networks- SNN (Statsoft®) software [33].

Because of its non-mechanistic, non-equilibrium and non-analytical behavior, ANNs have many limitations in terms of dynamic modeling, despite its accuracy in composition prediction. The performance of ANNs solely depends on its training and in addition, training requires a large set of experimental data to calibrate and evaluate the constant parameters of the neural network [1]. Thus, ANNs modeling may not be the viable option for a new technology such as biomass gasification as the number of experimental

data sets are limited. Even, any kind of open literature describing the ANNs modeling for downdraft biomass gasification was not found. However, MaurÃ-cio Bezerra et al. (2012) proposed an artificial neural network model for circulating fluidized bed gasifier and described the methods, results and validation in reference [33].

4 Experimental Investigation

Knowledge of experimental data of gasifier is one of the important aspects of modeling work. The experimental data is required to validate the model. Without validation of proposed model, further prediction and assessment on the model cannot be made and is not relevant. For the thesis work, the experimental data are collected mostly from two published literatures; Jayah et al.[34] and Bario et al. [35] as referenced.

The data collection mainly involves gathering of information on basic experimental setups, biomass properties, operating parameters such as moisture content, air to fuel ratio or equivalence ratio, temperature measured inside the gasifier, final composition of product gas and calorific heating value of the corresponding gas.

4.1 Experimental setups

A short review was performed on the basis of experimental setups of two experimental tests; Jayah et al. [34] and Barrio et al. [35]. The experimental setups are reviewed to identify the several setup parameters that can affect the gas production and drafted in table 4.1.

Table 4.1 Review on experimental setups of experimental tests

Parameters	Jayah et al.[34]	Barrio et al.[35]
Gasifier design	Downdraft gasifier	Downdraft gasifier
Fuel	Rubber wood	Pellets
Fuel size (cm)	3.5-5.5 cm	d=0.6 cm, l=0.6-1.5 cm
Capacity (kW_{th})	80	24.5-39.2
Diameter (m)	0.92	0.1
Length (m)	1.15	0.5
Gasification zone length (m)	0.220	0.250
Divergence angle	61^{o}	0
Thermocouple	12 type K & T	7 type-K
Gas analyser	Gas liquid chromatography (Carboxen 1000)	Gas chromatography (TCD detector, Carboxen 1000)

The schematic diagrams of the test gasifiers are also compared to each other in order to recognize the similarities and differences between the operational conditions.

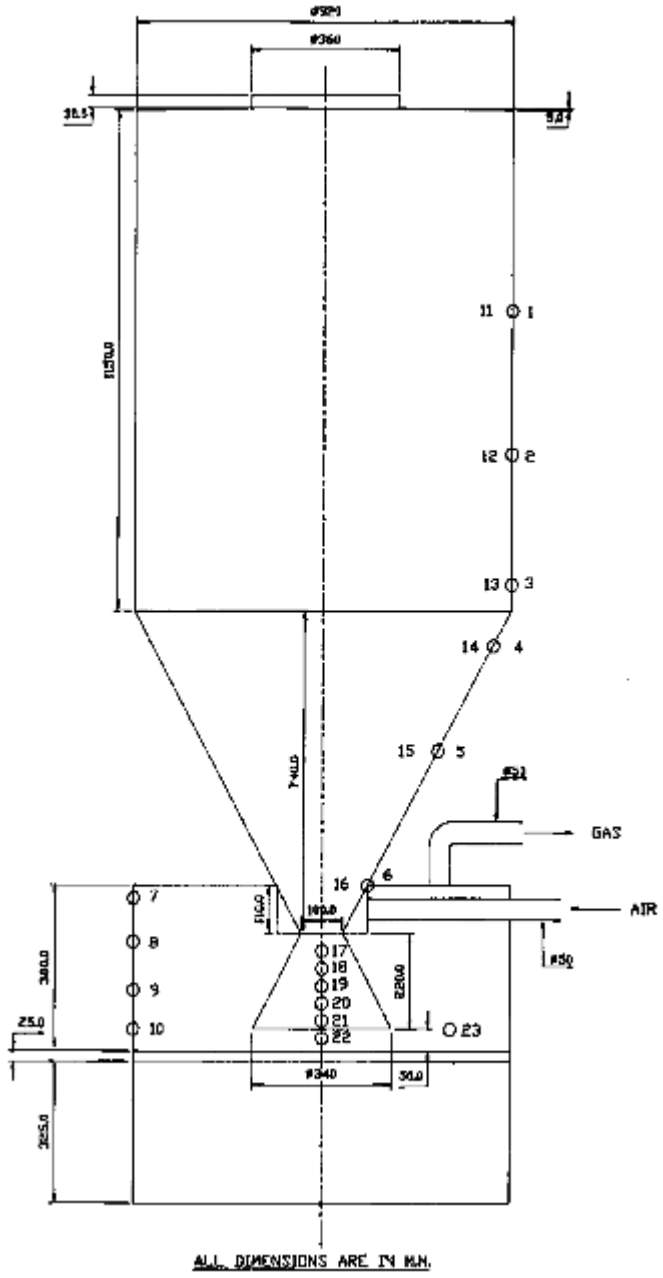

Figure 4.1 Schematic diagram of test gasifier from Jayah et al. test [34]

The apparent difference between the experimental set ups are the size of the test gasifiers and the divergence angle in the gasifier, which can be self-accessed from figure 4.1 and 4.2.

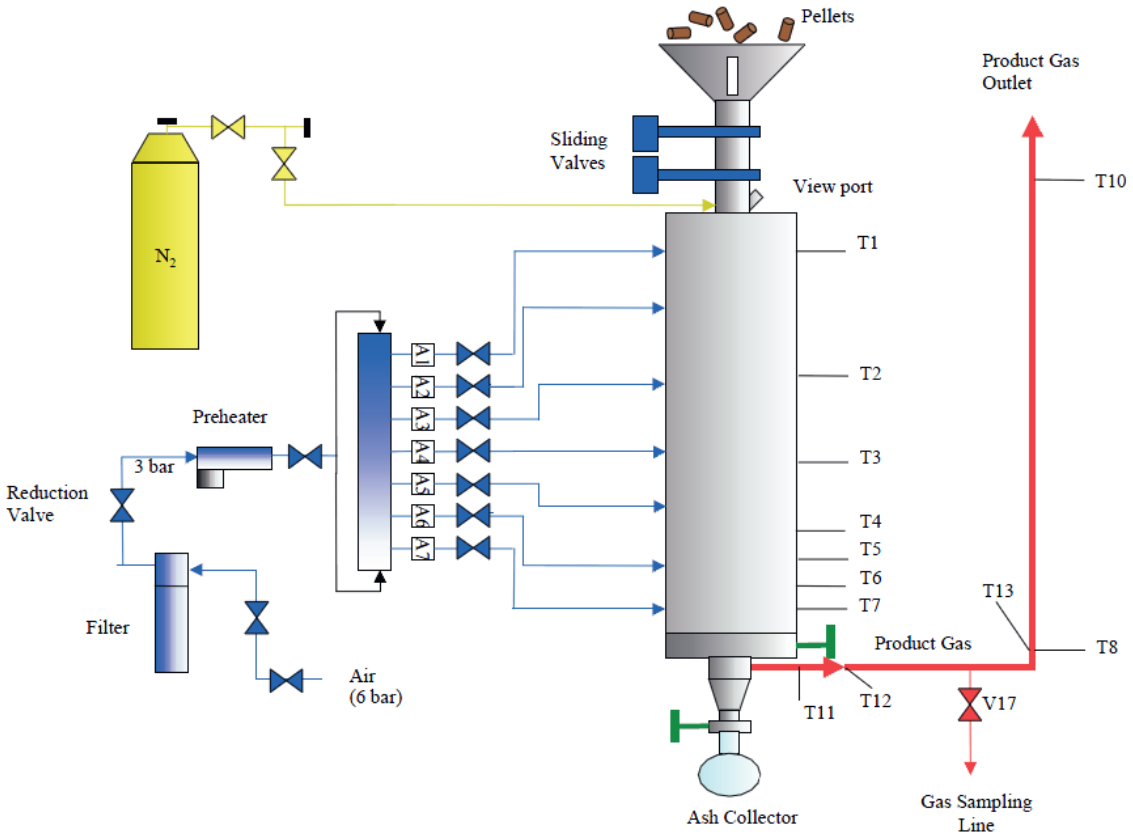

Figure 4.2 Schematic of test gasifier from Barrio et al. test [35]

4.2 Biomass properties

It is very essential to have knowledge about the properties of the feedstock as it provides thorough information on the possible mechanism of the process and helps to identify any possible risk on its utilization. Biomass is composed of carbon, hydrogen, oxygen, some traces of nitrogen & sulphur and inorganic impurities such as ash. Information regarding the elemental composition of biomass can be achieved from ultimate and proximate analysis of biomass. Ultimate analysis is the measurement of element composition in biomass, while proximate analysis is the measurement of volatile and non-volatile composition of biomass. However, present modeling requires only ultimate analysis properties of biomass material. In ultimate analysis of biomass, the composition of C, H N, S and ash are determined experimentally by chemical analysis, while the oxygen content (O) is determined as; O = [100-(C+H+N+S+ASH)]. The data collection of several biomass related properties from two referenced articles are summarized in Table 4.2.

Table 4.2 Properties of biomass

Parameters	Jayah et al.[34]	Bario et al.[35]
Biomass material	Rubber wood	Pellets
Ultimate analysis, daf		
C	50.6	50.7
H	6.5	6.9
N	0.2	< 0.3
O	42	42.4
Ash	0.7	0.39
Moisture content(MC) (%wt)	12.5-18.5	6.38-8
Energy content (MJ/kg)	19.6	18.86

4.3 Air to Fuel ratio

Air to fuel (A/F) ratio is the amount of air (in Nm^3 or kg) provided per unit mass (kg) of the fuel. In gasification process, supplied A/F ratio is always less than the stoichiometric A/F ratio as gasification only involves partial oxidation of the supplied biomass. Thus, the ratio of supplied A/F ratio to the stoichiometric A/F ratio gives the air to fuel equivalence ratio. The conventional sign for air to fuel equivalence ratio is λ, however most literatures also use the sign ϕ.

Air to fuel Equivalence ratio: $$\lambda = \frac{A/F_{supplied}}{A/F_{stoichiometric}} \tag{4.01}$$

In some literatures, equivalence ratio is taken with respect of fuel to air ratio. So, for the sake of brevity, present modeling work considers the equivalence ratio based on the air to fuel ratio. 0 values indicates complete absence of oxidant or oxygen, 1 refers to stoichiometric amount of oxidant and value more than 1 means presence of excess air in the system. The collected data on air to fuel ratio is summarized as in Table 4.3. The supplied A/F ratio for M. Barrio's experimental investigation is estimated with the help of Eq. (4.02) as the information were given based on air feeding rate and biomass feeding rate only. Air feeding rate

$$A/F_{supplied} = \frac{\text{Air feeding rate(kg/h)}}{\text{Biomass feeding rate(kg/h)}} \tag{4.02}$$

Table 4.3 Air to fuel ratio and equivalence ratio

Parameters	Jayah et al.[34]	Barrio et al.[35]
A/F $_{supplied}$ (kg_{air}/kg_{fuel})	1.86-2.37	1.45-1.70
A/F $_{stoichiometric}$ (kg_{air}/kg_{fuel})	6.22	5.877
Equivalence ratio	0.29-0.38	0.24-0.29

Thus, both experimental works were subjected to test the gasifier behavior with respect to different moisture content and A/F ratio as variables and study the consequences on gas composition, gasifier temperature and other parameters such as pressure drop and conversion efficiency.

4.4 Composition of product gas

The composition of product gas mainly consists of H_2, CO, CO_2, CH_4, H_2O and N_2. But the final compositions of product gas are mostly expressed on dry basis i.e. excluding the water content. The methods of gas analysis are described briefly in the respective referenced paper as present paper is concerned on the collected data rather than the procedure of measurements. The summary of gas analysis from Jayah et al. experiment is presented in Table 4.4 while from M. Bario is presented in Table 4.4.

Table 4.4 Gas composition (%) analysis from experimental tests by Jayah et al [34]

Test	MC $\%_{d.b}$	A/F ratio	ER	H_2	CO	CO_2	CH_4	N_2
T1	18.5	2.03	0.326	17.20	19.60	9.90	1.40	51.90
T2	16	2.2	0.353	18.30	20.20	9.70	1.10	50.70
T3	14.7	2.37	0.383	17.20	19.40	9.70	1.10	52.60
T4	16	1.96	0.315	17.00	18.40	10.60	1.30	52.70
T5	15.2	2.12	0.340	13.20	19.70	10.80	1.30	55.00
T7	14.7	1.86	0.299	15.50	19.10	11.40	1.10	52.90
T8	13.8	2.04	0.327	12.70	22.10	10.50	1.30	53,40

Table 4.5 Gas composition (%) analysis from several test runs by Barrio et al. [35]

Test	MC $\%_{d.b.}$	A/F ratio	ER	H_2	CO	CO_2	CH_4	N_2
#8b	7.25	1.536	0.261	16.8	25.8	9.1	1.5	46.8
#9	6.9	1.707	0.288	15.5	25.3	9.3	1.5	47.3
#12	7.02	1.684	0.284	16.4	25.2	9.4	1.5	47.5
#13a	6.38	1.66	0.281	15.6	23.9	10.1	1.7	48.7
#13b	8.0	1.52	0.258	17.2	26.4	8.8	1.4	46.3
#13c	7.58	1.454	0.247	16.4	25.2	9.4	1.5	47.5
#14	6.67	1.633	0.279	16.4	25.3	9.4	1.5	47.4

4.5 Temperature profile of gasifier

Temperatures were also recorded along different gasifier length with sets of several K- and T-types thermocouples. Experimental work of Jayah et al. describes the measurements of temperature from the reduction zone only as presented in the Figure 4.3. In the referenced article, the reduction zone is assumed to start from set point of divergence angle as shown in Fig (4.1). The temperatures were recorded during test 2, when the moisture content and equivalence ratio were 16% and 0.35 respectively.

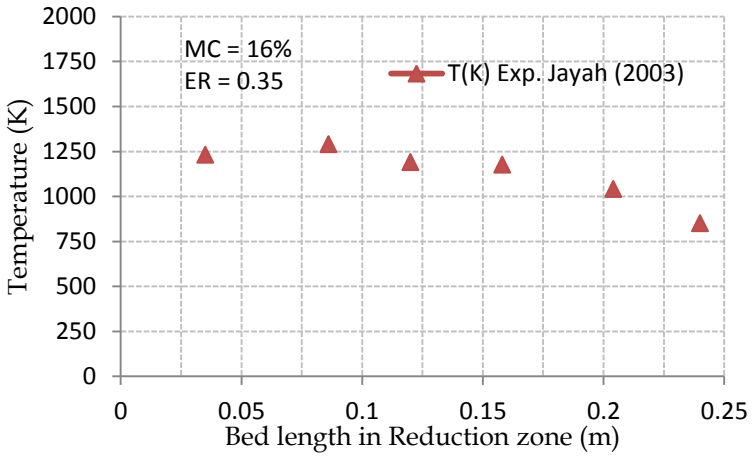

Figure 4.3 Temperature recorded along reduction zone [34]

Similarly, summary Barrio et al. paper reveals the measurements of gasifier temperature along the whole gasifier length and under several operating parameters such as moisture content and A/F ratio and is illustrated in Figure 4.4.

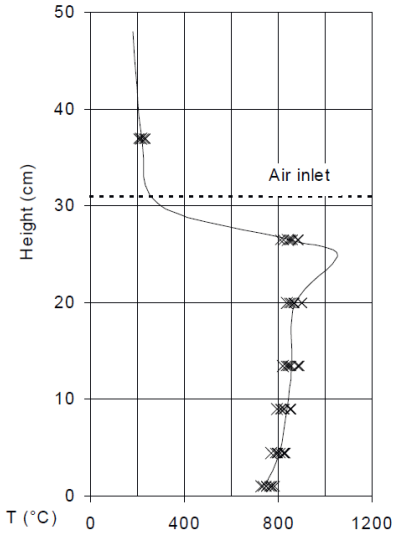

Figure 4.4 Experimental temperature profiles inside the gasifier [35]

5 Methods for Model Development

Development of a mathematical model requires a systematic approach with vivid outline and postulation of theories based on experimental works and assumptions. The main objective of any mathematical simulation is to create artificial system that is capable of performing similar action as that of the natural system with less effort and expense. The artificial system is the outcome of initial theories and assumptions. Thus, it is very essential and important to postulate the correct theory. For current model, following postulates are invoked:

- The objective of the simulation is to imitate the behavior of fixed bed downdraft gasifier.
- Wood based biomass is used as feedstock. Rubber wood is taken as sample for present model.
- Natural air (21% O_2, 79% N_2) is taken as gasification agent.
- Gasification process is considered to be auto-thermal i.e. absence of external heating source.
- Gasifier is partitioned into drying & pyrolysis zone, oxidation zone and reduction zone in a respective sequence.
- There is no heat exchange between various zones. [12]
- The overall heat loss from the gasifier is assumed to be related to both heating value of biomass and the equivalence ratio. It has been assumed that, heat loss is equal to the 10% of the product of equivalence ratio and the higher heating value (HHV) [12, 36].
- For simplicity, the product gas composition is supposed to be mixture of char (C), H_2, CO, CO_2, CH_4, H_2O and N_2, despite the evidence for formation of tar and other higher hydrocarbons.
- The composition of N_2 in product gas is not affected by the fuel nitrogen and N_2 does not participate in chemical reaction [7].
- Char is modeled as graphite carbon [12].
- It is assumed that at least 10% of char is always present in reduction zone to maintain the equilibrium of several char surface reactions [7].
- Chemical equilibrium exists among the gaseous species in all zones [28].
- The gasifier is considered to be one-dimensional [28].
- Gases in gasifier behave as an ideal gas [25].

After the postulation of main assumptions, a scheme for mathematical modeling is proposed. A schematic of present model scheme is presented in Figure 4.1. In the present modeling work, several gasifications related properties such as biomass properties, equivalence ratio and other have been identified and computed in accordance with the requirement of the model. Present model consists of three sub-model accounting for drying & pyrolysis,

oxidation and reduction zone. The output of pyrolysis zone is taken as input for oxidation zone. Similarly, the output of oxidation zone is taken as input for reduction zone. Sub-model for pyrolysis and oxidation zone are modeled using thermodynamic stoichiometric equilibrium approach while sub-model for reduction zone is modeled by finite kinetic approach.

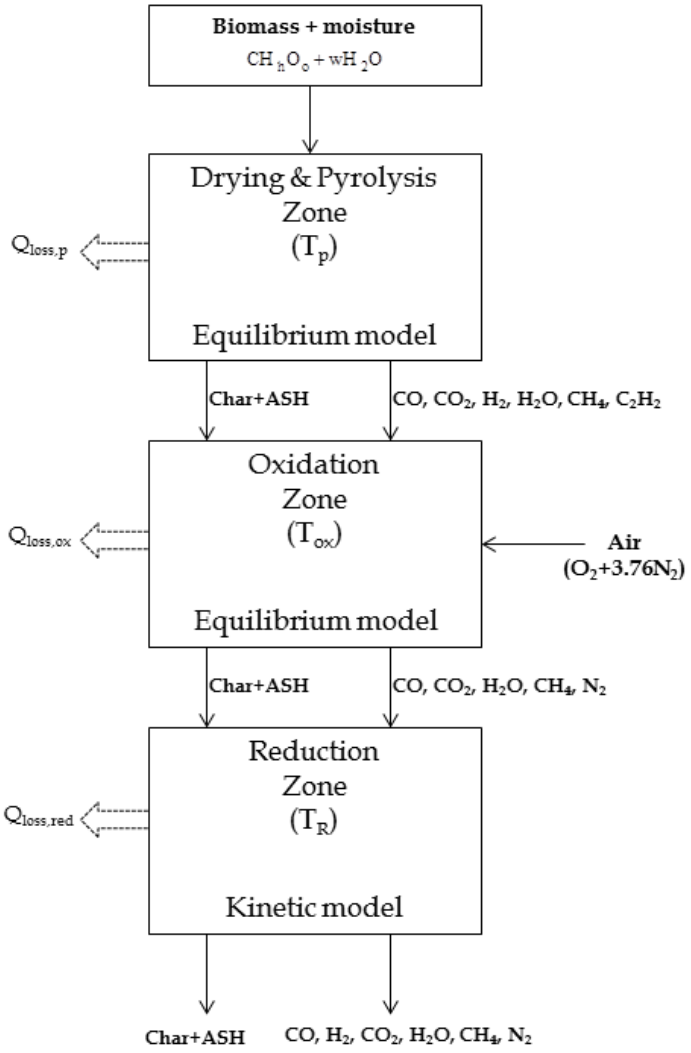

Figure 4.1 Three zone equilibrium and kinetic model of downdraft gasifier

Proposed postulations and scheme also demands proper tool for manipulation and computation of collected data. Computer software such as EXCEL, MATLAB, FORTRAN and similar mathematical applications are the convenient tools available commercially. For present work, EXCEL program with VBA (Visual Basis Application/Macros) have been selected which is capable of computing complex mathematical expression and furthermore, the user interface (UI) is easily understandable.

5.1 Gasification related properties

Properties of biomass and supplied air along with several operational properties such heat loss from gasifier are identified as gasification related properties. The parameters or values might not be in the format required by the model, thus it is very substantial and critical to manipulate the available data into the required format.

5.1.1 Biomass related properties

Biomass is a complex mixture of organic materials consisting of mainly carbon, hydrogen, oxygen, nitrogen on elemental basis. The corresponding elemental parameters can be achieved from the ultimate analysis of biomass. From the ultimate analysis of biomass, most of the biomass related properties could be identified such as chemical formula and heating value of the biomass.

Biomass chemical formula:

Despite the complexity to determine the chemical formula of biomass, several approximations have been imposed to generalize its chemical formula. One method is based on utilization of elemental composition from ultimate analysis of dry biomass and can be expressed as in Eq. (5.1-5.3) which is based on a single atom of carbon [5].

Biomass (typical chemical formula) = $C_cH_hO_o$

$$c = 1 \tag{5.01}$$

$$h = \frac{H_{\%} \times M_C}{C_{\%} \times M_H} \tag{5.02}$$

$$o = \frac{O_{\%} \times M_C}{C_{\%} \times M_O} \tag{5.03}$$

C%, H% and O% are the compositional percent of carbon, hydrogen and oxygen acquired from the ultimate analysis of dry biomass. Table 5.1 summarizes properties of biomass based on ultimate analysis of typical biomass used in gasifier and their chemical formula.

Table 5.1 Ultimate analysis of several biomasses and their chemical formula [37], [38], [35]

	Ultimately Analysis (%)					$C_cH_hO_o$		
Biomass	C	H	N	Ash	O	c	h	o
Pellet	50.7	6.9	0.3	0.39	41.71	1	1.621	0.617
Rubber Wood	50.6	6.5	0	0.7	42.2	1	1.530	0.626
Eucalyptus	46.04	5.82	0	3.35	44.79	1	1.506	0.730
Dry Subabul	48.15	5.87	0.03	1.2	44.75	1	1.452	0.697
Forest residue chips	51.3	6.1	0.4	1.3	40.9	1	1.417	0.598
Spruce bark	49.9	5.9	0.4	2.3	41.5	1	1.409	0.624
Wood chips	51.8	6.1	0.3	0.6	41.2	1	1.403	0.597
Saw dust (Pine)	51.00	6.00	0.08	0.08	42.84	1	1.402	0.630
Coconut shell	52.00	5.70	0.04	2.10	43.80	1	1.306	0.632
Douglas Fir bark	56.2	5.9	0	1.2	36.7	1	1.251	0.490

Moisture content:

Moisture content of biomass is usually presented in weight fraction (wt.%). However, amount of water per kmol of wood biomass is required for stoichiometric calculation. When the moisture content (*MC*) of wood biomass is known, the amount of water (*w*) can be determined by following derivation [7]:

$$\mathrm{MC} = \frac{\mathrm{m_{water}}}{\mathrm{m_{biomass}}} \times 100\% = \frac{\mathrm{m_{water}}}{\mathrm{m_{dry\_biomass}} + \mathrm{m_{water}}} \times 100\% = \frac{\mathrm{wM_{water}}}{\mathrm{nM_{biomass}} + \mathrm{wM_{water}}} \times 100\%$$

Finally,

$$\mathrm{w} = \frac{\mathrm{M_{biomass}} \times \mathrm{MC}}{\mathrm{M_{water}}(1 - \mathrm{MC})} \tag{5.04}$$

The molecular mass of biomass is estimated as:

$$\mathrm{M_{biomass}} = \mathrm{M_C} \times \mathrm{c} + \frac{\mathrm{M_H}}{2} \times \mathrm{h} + \frac{\mathrm{M_O}}{2} \times \mathrm{o} \tag{5.05}$$

where M_C, M_H and M_O are the molecular mass of carbon, hydrogen and oxygen.

Let the rubber wood biomass be considered to have moisture content of 16% by weight, and then from Eq. (5.04), w for rubber wood is estimated to be 0.249.

Heating value:

Heating value of biomass is the amount of the heat released during its complete combustion. There are various approaches to calculate the heating value of the biomass such as experimental methods and unified correlation approach based on ultimate analysis of biomass. Heating value of biomass is dependent to its moisture content. Since the moisture content is one of the prominent variables in present gasifier model, it is not relevant to abstract the experimental heating value of the biomass. Thus, heating value may be calculated using several correlations as described in table 5.2.

Table 5.2 Correlation for estimation of HHV of solid fuel [37]

Name of investigator	Correlation	Value (MJ/kg)	Basis and Accuracy
Dulong's (1880)	0.3383C + 1.443(H - O/8) + 0.0942S	18.88	derived from coal properties (~5-7% error)
Strache and Lant (1924)	0.3406C + 1.4324H - 0.1532O + 0.1047S	20.08	modified version of Dulong's (~2% error)
Seyler (1938)	0.519C + 1.625H + 0.001O²- 17.87	20.73	HHV as a function of C, H,O (~1%error)
Tillman (1978)	0.4373C - 1.6701	20.46	HHV for biomass as a function of C (~5% error)
Jenkins (1985)	-0.763+ 0.301C + 0.525H + 0.064O	20.58	for biomass (~7% error)

The values for C, H, O and S are retrieved form ultimate analysis of dry biomass. Thus obtained heating value is the highest heating value that can be received from the combustion of biomass as it accounts for the dry biomass i.e. without water/moisture. Investigator of these correlations also claimed the accuracy of their correlation for predicting the heating value of the solid fuels. However, most of the correlations projects heating value in a narrow range. So, correlation proposed by Seyler has been incorporated in present modeling.

$$\text{Seyler: } HHV = 0.519C + 1.625H + 0.001O^2 - 17.87 \text{ (MJ/kg)} \quad (5.06)$$

As the computation of whole model is based on unit mole of biomass, the unit of HHV is converted into MJ/kmol with the following expression:

$$HHV(kJ/kmol) = HHV(MJ/kg) \times M_{biomass}(kg/kmol) \times 1000 \quad (5.07)$$

Using the above mentioned correlation, HHV of Rubber wood is calculated as 20.73 MJ/Kg or 488733.034 KJ/Kmol. Thus, calculated HHV for Rubber wood is almost 3.5% higher as mentioned by Jayah et al. and can be supported by the fact that the Seyler correlation accounts HHV for completely dry biomass.

Heat of formation of biomass

Heat of formation of biomass is considered as the heat required to form the bond between carbon, hydrogen and oxygen as mention in the chemical formula of biomass. The simplest approach to estimate the heat of formation of biomass may be proceeded by modeling a generic reaction for formation of biomass as described in Eq. (5.08) [7].

$$C + 0.76H_2 + 0.31O_2 \rightarrow CH_{1.53}O_{0.626} \text{ (Rubber wood)} \tag{5.08}$$

The heat of formation of biomass can be determined by employing Hess's Law. Hess's law states that *ΔH for a reaction can be found indirectly by summing ΔH values for any set of reactions which sum to the desired reaction*. It can also be supported by the fact that enthalpy is a state property, so ΔH is independent of path. The computational approach to estimate the heat of formation of biomass is described in Appendix A1. Thus, the heat of formation of Rubber wood is estimated to be -89854.0977 kJ/kmol.

Specific heat of biomass

Specific heat of biomass is an essential thermodynamic property often required during thermodynamic calculations. Specific heat of biomass is found to be dependent on temperature and moisture content which can be estimated using several correlations. For example, correlation described by Thunman et al. can be presented as following [39]:

$$c_{p,dry} = 2.45T + 531.2 \text{ (kJ/kg·K)}$$

$$c_{p,wet} = \frac{\left(c_{p,dry} + 4190\frac{MC}{1-MC}\right)}{\left(1+\frac{MC}{1-MC}\right)} + \left(23.55T - 1320\frac{MC}{1-MC} - 6191\right)\frac{MC}{1-MC} \text{ (kJ/kg·K)} \tag{5.09}$$

Likewise, specific heat of dry wood can also be described by correlation given by TenWolde et al. [40, 41] as is written as as follows:

$$c_{p,dry} = 0.1031 + 0.003867T \text{ (kJ/kg·K)}$$

$$c_{p,wet} = \frac{\left[c_{p,dry} + 4.19MC\right]}{(1+MC)} + (0.02355T - 1.32MC - 6.191) \times MC \ \ (kJ/kg{\cdot}K) \tag{5.10}$$

Based on the referenced literature, the calculated c_p has a unit of J/kg.K. Due to the requirement of the model, thus calculated c_p is reformatted into KJ/Kmol.K by following expression.

$$c_{p,wet}(kJ/kmol.K) = c_{p,wet}(J/kg.K) \times M_{biomass}(kg/kmol)/1000 \tag{5.11}$$

Table 5.3 Estimated specific heat of wood derived from different correlations.

	Thunman et al. [39]	TenWolde et al.[41]
$C_{p,dry}$ (kJ/kg.K)	1.2616	1,2560
$C_{p,wet}$ (kJ/kg.K)$_{MC=10\%}$	1.630	1.5926
$C_{p,wet}$ (kJ/kmol.K)	38,431	37.539

Both of the correlations estimate the specific heat of wood of same range and either can be employed in the current model. However,

5.1.2 Equivalence ratio

Equivalence ratio refers to the ratio of supplied air to fuel ratio to stoichiometric air to fuel ratio:

Air to fuel Equivalence ratio (ER): $\lambda = \dfrac{A/F_{supplied}}{A/F_{stoichiometric}}$

$A/F_{supplied}$ is also a operational parameter for current model. It can also be manipulated accordingly, while $A/F_{stoichiometric}$ is a constant for a biomass material and can be calculated from Eq. (5.11) [42].

$$A/F_{stoichiometric} = \left(1 + \frac{h}{4} - \frac{o}{2}\right) \times \left(\frac{M_{O_2} + 3.76M_{N_2}}{M_{biomass}}\right) \ (kg_{air}/kg_{biomass}) \tag{5.12}$$

where $\left(1 + \dfrac{h}{4} - \dfrac{o}{2}\right)$ refers to stoichiometric amount of oxygen required for complete combustion on molar basis which is the cumulative oxygen required by 1 mole of biomass. For instance, the numerical value 1 indicates the oxygen

consumed by 1 mole of carbon in biomass ($C_1H_hO_o$), h/4 refers to oxygen required for oxidation of fuel hydrogen and O/2 is the oxygen content in the biomass and is subtracted from the total oxygen need. M_{O2} and M_{N2} are molecular weight of oxygen and nitrogen.

The $A/F_{stoichiometric}$ ratio for rubber wood is estimated to be 6.23 kg_{air}/kg_{fuel}, and considering variable $A/F_{supplied}$ to a value of 2.2 kg_{air}/kg_{fuel} results to value of 0.353 for air to fuel equivalence ratio.

When equivalence ratio for a provided condition is known, then it is possible to estimate the amount of air supplied on molar basis as demanded by the stoichiometric equations that can be calculated with following expression [28]:

$$a = \left(1 + \frac{h}{4} - \frac{o}{2}\right) \times \lambda \tag{5.13}$$

Thus, for a equivalence ratio of 0.353, the amount of air supplied is estimated to be 0.377 mole.

5.1.3 Heat loss

Inclusion of heat loss in a simulation is optional. However, implementing the theory of heat loss from the gasifier may provide better comprehension over energy balance and in real test scenario, heat loss from the gasifier is inevitable. Estimating the heat loss from gasifier is very crucial as the temperature of the gasifier varies with other operational parameters such as moisture content, equivalence ratio, which refers to amount of air (oxygen) supplied and heating value of biomass. Thus, empirical assumption for heat loss would provide great assist during simulation of gasification process. From the experimental results, for the biomass with HHV in the range of 15-20 MJ/kg and operational equivalence ratio of 0.25-0.45, the overall heat loss has been observed to vary in the range of 3-6% [12]. Thus, the overall heat loss is assumed to be 10% of the product of equivalence ratio and HHV [36]. Since the heat loss is modeled as a function of equivalence ratio and equivalence ratio is operational parameter of oxidation sub-model, the heat loss is accounted only in oxidation sub-model.

5.2 Formulation of pyrolysis sub-model

Sub-model of drying and pyrolysis are approached through thermodynamic stoichiometric equilibrium modeling. Formulation of pyrolysis zone sub-model is based on empirical assumptions that have been supported by the

experimental results of biomass pyrolysis [12]. According to the postulates, the chemical reaction that governs the pyrolysis zone is written as:

$$CH_hO_o + wH_2O \rightarrow n_{p,C}C + n_{p,CO_2}CO_2 + n_{p,CO}CO + n_{p,CH_4}CH_4 + n_{p,H_2}H_2 + n_{p,C_2H_2}C_2H_2 + n_{p,H_2O}H_2O \quad (5.14)$$

As rubber wood($C_1H_{1.53}O_{0.626}$) has been chosen as sample biomass for present modeling work, the parameter such as h(1.53), o(0.626) and w(0.249) have known values.

Rewriting the constituent balance of pyrolysis reaction, we have;

Carbon balance: $n_{p,C} + n_{p,co} + n_{p,co_2} + n_{p,CH_4} + 2n_{p,C_2H_4} = 1$ (5.15)

Hydrogen balance: $2n_{p,H_2} + 4n_{p,CH_4} + 2n_{p,H_2O} + 2n_{p,C_2H_2} = 2w + h$ (5.16)

Oxygen balance: $n_{p,co} + 2n_{p,co_2} + n_{p,H_2O} = w + o$ (5.17)

Several assumptions for current pyrolysis zone model have been drafted which is based on the fact that the affinity between H and O is much higher than that of C and O [12]. The fate of pyrolysis products are mainly governed by the initial association of C,H and O with each other during formation of biomass. The association of C, H and O also determines the HHV of biomass [37] and the same assumptions on association of C, H, O can be employed to estimated the composition of pyrolysis products. The assumptions are invoked as follows:

- 80% (4/5) of fuel oxygen (O) is associated with fuel hydrogen (H) in the form of H_2O [37].
- 20% (1/5) of fuel oxygen (O) is associated with fuel carbon (C) and releases as CO and CO2 [37].
- The ratio of mol of CO and CO_2 is inversely related with their molecular mass. i.e. [12, 43],

$$\frac{n_{CO}}{n_{CO_2}} = \frac{44}{28} \quad (5.18)$$

- 50% of available hydrogen in fuel releases as H_2 on decomposition [43].
- Remaining 50% of available hydrogen in fuel is released in the form of CH_4 and C_2H_2 [43].
- The ratio of mol of CH_4 and C_2H_2 is inversely related with their molecular mass i.e. [43],

$$\frac{n_{CH_4}}{n_{C_2H_2}} = \frac{26}{16} \tag{5.19}$$

Formulation of these assumptions into mathematical model is shown in Appendix C1. And an alternative method to estimate these value employ the VBA programmatic "Goal Seek Function" in EXCEL which is shown in Appendix D1. Thus, the final estimated composition of pyrolysis zone is summarized in Table 4.3.

Table 4.3 Composition of Pyrolysis product (MC = 18.5%, ER = 0.326)

	$n_{p,C}$	n_{p,CO_2}	$n_{p,CO}$	n_{p,CH_4}	n_{p,H_2}	n_{p,C_2H_2}	n_{p,H_2O}
$n_{p,i}$(mol)	0.797	0.035	0.055	0.051	0.132	0.031	0.798
$y_{p,i}$(%)	41.98	1.838	2.889	2.662	6.963	1.638	42.022

After the successful computation of composition of pyrolysis product, the temperature of pyrolysis zone is predicted using thermodynamic equilibrium approach. The energy balance equation can be retrieved from Eq. (2.21) as:

$$\left[h_f^0 + c_p\Delta T\right]_{wood} + w\left[h_{f,(l)}^0 + c_p\Delta T\right]_{H_2O} = \begin{bmatrix} n_C.h_{f,C}^0 + n_{H_2}h_{f,H_2}^0 + n_{co}h_{f,CO}^0 + n_{co_2}h_{f,CO_2}^0 \\ + n_{CH_4}h_{f,CH_4}^0 + n_{C_2H_2}h_{f,C_2H_2}^0 + n_{H_2O}h_{f,H_2O}^0 \end{bmatrix}_P$$
$$+ \Delta T\left[n_C c_{p,C} + n_{H_2}c_{p,H_2} + n_{co}c_{p,CO} + n_{co_2}c_{p,CO_2} + n_{CH_4}c_{p,CH_4} + n_{C_2H_2}c_{p,C_2H_2} + n_{H_2O}c_{p,H_2O}\right]_P + Q_p \tag{5.20}$$

In this expression, the heat of formation of biomass is calculated form Eq. (5.08), c_p from Eq. (5.09 or 5.10) and heat of formation ($h_{f,i}^0$) of various elements and compounds from thermodynamic table as mentioned in Appendix B1. The heat loss value is taken from Table 4.2. Likewise, c_p (heat capacity) for each element can be estimated by the following relation [7].

$$c_p = R\left(A + BT_{am} + \frac{C}{3}\left(4T_{am}^2 - T_{atm}T_P\right) + \frac{D}{T_{atm}T_P}\right) \tag{5.21}$$

where, $T_{am} = \frac{T_{atm} + T_P}{2}$ and $\Delta T = T_P - T_{atm}$

The values of thermodynamic constant A, B, C & D are also retrieved from Appendix B1. These energy balance expression contains only one unknown parameter, which is temperature of pyrolysis (T_P). The solution of these sophisticated expressions is achieved by implementation of *"Goal seek Function"* in EXCEL. The procedures are well explained in Appendix D1.

At last, the temperature of pyrolysis zone for rubber wood biomass with 16% moisture content is estimated to be **701.81 K** or **428.66 °C** from the utilization of energy balance equation.

5.3 Formulation of Oxidation sub-model

Oxidation zone sub-model is drafted based on thermodynamic stoichiometric equilibrium approach. The notion of oxidation zone involves partial oxidation of pyrolysis product as input in presence of non-stoichiometric amount of air/oxidant. The generic reaction stoichiometry during oxidation of pyrolysis product can be rewritten as:

$$n_{p,C}C + n_{p,CO_2}CO_2 + n_{p,CO}CO + n_{p,CH_4}CH_4 + n_{p,H_2}H_2 + n_{p,C_2H_2}C_2H_2 + n_{p,H_2O}H_2O +$$
$$a(O_2 + 3.76N_2) \rightarrow n_{ox,C}C + n_{ox,CO_2}CO_2 + n_{ox,CO}CO + n_{ox,CH_4}CH_4 + n_{ox,H_2O}H_2O + 3.76aN_2$$

From the element balance of oxidation reaction, we get;

Carbon balance: $n_{p,C} + n_{p,co} + n_{p,co_2} + n_{p,CH_4} + 2n_{p,C_2H_4} = n_{ox,C} + n_{ox,co} + n_{ox,co_2} + n_{ox,CH_4}$ (5.22)

Hydrogen balance: $2n_{p,H_2} + 4n_{p,CH_4} + 2n_{p,H_2O} + 2n_{p,C_2H_2} = 4n_{ox,CH_4} + 2n_{ox,H_2O}$ (5.23)

Oxygen balance: $n_{p,co} + 2n_{p,co_2} + n_{p,H_2O} + 2a = n_{ox,co} + 2n_{ox,co_2} + n_{ox,H_2O}$ (5.24)

Such generic modeled reactions are sufficient enough to describe the composition of final products but these modeled reactions may not provide a vivid comprehension of reaction mechanisms and reaction pathways. Thus, equilibrium modeling requires empirical assumptions for consumption of pyrolysis products.

Oxidation zone sub-model also engages several postulates, to simplify the complexity of partial oxidation. One of the drawbacks of equilibrium modeling is that it embodies many assumptions that may yield great disagreement under various circumstances [3]. However, the simplest approach is to invoke postulates that would assist to simulate the actual process. Thus, following assumptions are adapted for oxidation sub-model:

- Hydrogen from the pyrolysis zone is fully oxidized to H_2O due to its reactivity with oxygen and high burning velocity [12, 44].
- Balanced oxygen oxidizes C_2H_2 or it can be assumed that acetylene is carried forward to reduction zone as well [44, 45].

- The remaining oxygen is consumed in char oxidation. It is because of larger reaction area available for O_2 adsorption on highly reactive pyrolysis char and produces CO and CO_2 [44, 45].
- The ratio of formation of CO and CO_2 is inversely proportional to the exothermicity of their reactions. i.e. [45],

$$\frac{n_{CO}}{n_{CO_2}} = 3.5606 \tag{5.25}$$

- CO, CO_2 and H_2O formed during the pyrolysis are added to the composition of oxidation zone.
- CH_4 is carried forward to the reduction zone due to their low burning velocity and lack of oxygen [12].
- N_2 present in air does not participate in chemical reaction.

Several equations are formulated from these empirical assumptions and solved to determine the compositions of oxidation products, which are show in Appendix C2.

An alternative approach to solution of this computation is convenient by the application of VBA programmatic "Goal Seek Function" in EXCEL, which is described in Appendix D1. Thus, the final predicted composition of oxidation zone is listed in Table 4.4.

Table 4.4 Composition of Oxidation product (MC = 18.5%, ER = 0.326)

	$n_{ox,C}$	n_{ox,CO_2}	$n_{ox,CO}$	n_{ox,CH_4}	n_{ox,H_2O}	n_{ox,N_2}
$n_{ox,i}$ (mol)	0.462	0.170	0.317	0.051	0.961	1.310
$y_{ox,i}$ (%)	14.11	5.22	9.69	1.55	29.38	40.05

The temperature of oxidation zone is possible to determine by thermodynamic equilibrium approach for energy balance of oxidation zone. The energy balance of oxidation zone can be re-expressed as:

$$\begin{bmatrix} n_C h^0_{f,C} + n_{H_2} h^0_{f,H_2} + n_{co} h^0_{f,CO} + n_{co_2} h^0_{f,CO_2} \\ + n_{CH_4} h^0_{f,CH_4} + n_{C_2H_2} h^0_{f,C_2H_2} + n_{H_2O} h^0_{f,H_2O} \end{bmatrix}_P + \Delta T \begin{bmatrix} n_C c_{p,C} + n_{H_2} c_{p,H_2} + n_{co} c_{p,CO} + n_{co_2} c_{p,CO_2} \\ + n_{CH_4} c_{p,CH_4} + n_{C_2H_2} c_{p,C_2H_2} + n_{H_2O} c_{p,H_2O} \end{bmatrix}_P =$$

$$\begin{bmatrix} n_C h^0_{f,C} + n_{co} h^0_{f,CO} + n_{co_2} h^0_{f,CO_2} + n_{CH_4} \\ h^0_{f,CH_4} + n_{H_2O} h^0_{f,H_2O} + a h^0_{f,O_2} + 3.76 a h^0_{f,N_2} \end{bmatrix}_{ox} + \Delta T \begin{bmatrix} n_C c_{p,C} + n_{co} c_{p,CO} + n_{co_2} c_{p,CO_2} + n_{CH_4} \\ c_{p,CH_4} + n_{H_2O} c_{p,H_2O} + a c_{p,O} + 3.76 a c_{p,N_2} \end{bmatrix}_{ox} + Q_{ox}$$

The solution to this complex equation is approached in a similar fashion as done for energy balance of pyrolysis. The constants are referred from thermodynamic table as mentioned in Appendix B1. Likewise, the heat loss value is taken from Table 4.2 and c_p (heat capacity) for each element can be estimated by the following relation:

$$c_p = R\left(A + BT_{am} + \frac{C}{3}\left(4T_{am}^2 - T_{ox}T_P\right) + \frac{D}{T_{ox}T_P} \right) \tag{5.26}$$

where $T_{am} = \frac{T_{ox} + T_P}{2}$ and $\Delta T = T_{ox} - T_P$

Finally, the unknown parameter T_{ox} is estimated by execution of *"Goal seek Function"* in EXCEL. The oxidation temperature is predicted to be **1256.45 K** or **983.30 °C** by using energy balance equation.

5.4 Formulation of Reduction sub-model

Reduction zone was formulated based on finite kinetic approach, which is based on the model proposed by Giltrap et al. [25]. The net formation or destruction of any gaseous species is modeled based on their kinetics as a function of length of reduction zone. Thus, reduction zone is partitioned into n number of compartments of length Δz = 0.001 mm. Present kinetic sub-model for reduction zone also enables to evaluate the effect of several variables such as superficial velocity, temperature and pressure on the final composition of the product gas. The final products from oxidation sub-model are considered as input for the first section (n = 1) in reduction sub-model and the gas composition along with other parametrics at n = 250 i.e. at the length of 0.25 m is determined.

As described in section 3.2.3, the net creation or destruction of any chemical species may be modeled as Eq. (3.38) and is rewritten as [25]:

$$\frac{dn_x}{dz} = \frac{1}{v}\left(R_x - n_x \frac{dv}{dz} \right)$$

It is apparent that no. of mol of any gaseous species at z^{nth} compartment is dependent to rate of formation of corresponding species (R_x) and gas flow (v).

Furthermore, the rate of formation of gaseous species participating in gasification reaction is determined by the rate of modeled reaction for reduction zone. If Eq. (3.01-3.04) are considered to be modeled reaction for present simulation, then the estimation of rate of formation of gaseous species are described in table 3.4. Moreover, the rate of modeled reaction and associated kinetic parameters are displayed in table 4.5.

Table 4.5 Gasification reactions and kinetic parameter [25]

	Reaction	Reaction rate (mol/m^3.s)	A_i (1/s)	E_i (kJ/mol)
R1	Boudouard reaction: $C + CO_2 \leftrightarrow 2CO$	$r_1 = C_{RF} A_1 \exp\left(\frac{-E_1}{RT}\right) \cdot \left(y_{CO_2} - \frac{y_{CO}^2}{K_{eq,1}}\right)$	3.616 x 10^1	77.39
R2	Water-gas reactions: $C + H_2O \leftrightarrow CO + H_2$	$r_2 = C_{RF} A_2 \exp\left(\frac{-E_2}{RT}\right) \cdot \left(y_{H_2O} - \frac{y_{CO} \cdot y_{H_2}}{K_{eq,2}}\right)$	1.517 x 10^4	121.62
R3	Methane formation: $C + 2H_2 \leftrightarrow CH_4$	$r_3 = C_{RF} A_3 \exp\left(\frac{-E_3}{RT}\right) \cdot \left(y_{H_2}^2 - \frac{y_{CH_4}}{K_{eq,3}}\right)$	4.189 x 10^{-3}	19.21
R4	Steam reformation: $CH_4 + H_2O \leftrightarrow CO + 3H_2$	$r_4 = A_4 \exp\left(\frac{-E_4}{RT}\right) \cdot \left(y_{CH_4} \cdot y_{H_2O} - \frac{y_{CO} \cdot y_{H_2}^3}{K_{eq,4}}\right)$	7.301 x 10^{-2}	36.15

The rate of char surface reaction is also dependent on char reactivity and may be incorporated into present simulation by multiplying the rate of char surface reaction by char reactivity factor (C_{RF}) [25, 27]. The overall rate of gasification reaction is also dependent on the gasifier temperature at z^{nth} section and chemical equilibrium constants of individual gasification reactions, which can be calculated as[25]:

$$\frac{dT}{dz} = \frac{1}{v \cdot \sum_x n_i c_{p,i}} \left(-\sum_i r_i \Delta H_i - v\frac{dP}{dz} - P\frac{dv}{dz} - \sum_i R_i c_{p,i} T \right) \tag{5.27}$$

$$\ln K_{eq,j} = -\frac{J}{RT} + \Delta A \cdot \ln T + \frac{\Delta B}{2} T + \frac{\Delta C}{6} T^2 + \frac{\Delta D}{2T^2} + I \tag{5.28}$$

where P is pressure, R is gas constant and I,J,A,B,C,D are thermodynamic constants and its estimation is described in Appendix C1. Furthermore, the rate of formation of any species and temperature of gasifier is affected by the gas flow rate and pressure at z^{nth} section. So, the gas velocity and pressure at z^{nth} section can be determined as followings [25]:

$$\frac{dv}{dz} = \frac{1}{\sum_i n_i c_{p,i}} \left(\frac{\sum_i n_i c_{p,i} \sum_i R_i}{n} - \frac{\sum_i r_i \Delta H_i}{T} - \frac{dP}{dz}\left(\frac{v}{T} + \frac{v\sum_i n_i c_{p,i}}{P}\right) - \sum_i R_i c_{p,i} \right) \tag{5.29}$$

$$\frac{dP}{dz} = 1183\left(\rho_{gas}\frac{v^2}{\rho_{air}}\right) + 388.19v - 79.896 \quad [27] \tag{5.30}$$

where v is the gas velocity, ρ_{gas} is the density of gaseous species from reduction zone and ρ_{air} is the density of air. Thus, the simultaneous computation of Eq. (3.38) and Eq. (5.27-5.30) would yield the composition of any gaseous species at n^{th} section and the computational methods are described in Appendix C3. The product gas composition of reduction zone is shown in table 4.5.

Table 4.5 Composition of Reduction product (MC = 18.5%, ER = 0.326)

	n_{ox,H_2}	n_{ox,CO_2}	$n_{ox,CO}$	n_{ox,CH_4}	n_{ox,H_2O}	n_{ox,N_2}
$n_{ox,i}$ (mol)	0.458	0.298	0.697	0.051	0.835	1.722
$y_{ox,i}$ (%)	11.29	7.34	17.17	1.26	20.55	42.39

Thus, a mathematical model based on thermodynamic stoichiometric equilibrium and finite kinetic approach is modeled, which has a considerable competence for prediction of product gas composition, calorific heating value, cold gas efficiency and temperature of each zone. This model also enables the researcher to study the influence of moisture content, air to fuel ratio and different biomass source on composition of product gas, its heating value and temperature.

6 Results

The final measurements displays that the product gas composition consists of H_2, CO, CO_2, CH_4, N_2 and H_2O. From utilization perspective, the product gas composition is deliberated as dry gas mixture. However, N_2 cannot be discarded as it plays a major role in dilution of product gas. The experimental product gas composition in most of the referenced articles, are given on dry basis. So, it is quite relevant to express the present gas composition on dry basis for comparison and validation of dry gas composition. And dry gas composition is estimated with the help of Eq. (6.01) as expressed below:

$$y_{n_i,db} = \frac{y_{n_i\,wb}\%}{(100 - MC\%)} \times 100\% \tag{6.01}$$

Thus, the final dry molar compositions ($y_{ni,d.b}$) of the product gas obtained from gasification of rubber wood are estimated, and are displayed in Table 6.1. Likewise, $m_{ni,d.b}$ represents the dry mass fraction ($m_{f,ni}$) of gas composition that are employed to calculate the carbon conversion during the gasification process, and are calculated as:

$$m_{n_i}(g) = n_i(mol) \times M_i(g/mol) \tag{6.02}$$

$$m_{f,n_i\,(db)} = \frac{m_{n_i}}{\sum_i m_{n_i}} \times 100\% \tag{6.03}$$

Table 6.1 Final composition at the end of reduction zone for Rubber wood (MC=18.5%, ER=0.326)

	H_2	CO	CO_2	CH_4	N_2	H_2O
n_i (mol)	0.458	0.697	0.298	0.051	1.72	0.8351
m_i(g)	0.925	19.533	13.11	0.82	48.24	15.04
y_{ni} (%)	11.29	17.17	7.37	1.26	42.39	20.55
$m_{f,ni}$(%) (d.b)	1.12	23.64	15.87	0.99	58.38	
y_{ni}(%) (d.b)	14.22	21.61	9.23	1.59	53.36	

Furthermore, the dry gas composition from rubber wood is schematically compared with the dry gas composition obtained from pellets as in Figure 6.1. The compositions of product gas from rubber wood and pellets vary notably because of anisotropic biomass chemical composition. Thus, it is very essential to have knowledge on ultimate analysis of biomass, as they have the potentiality to change the fate of product gas composition.

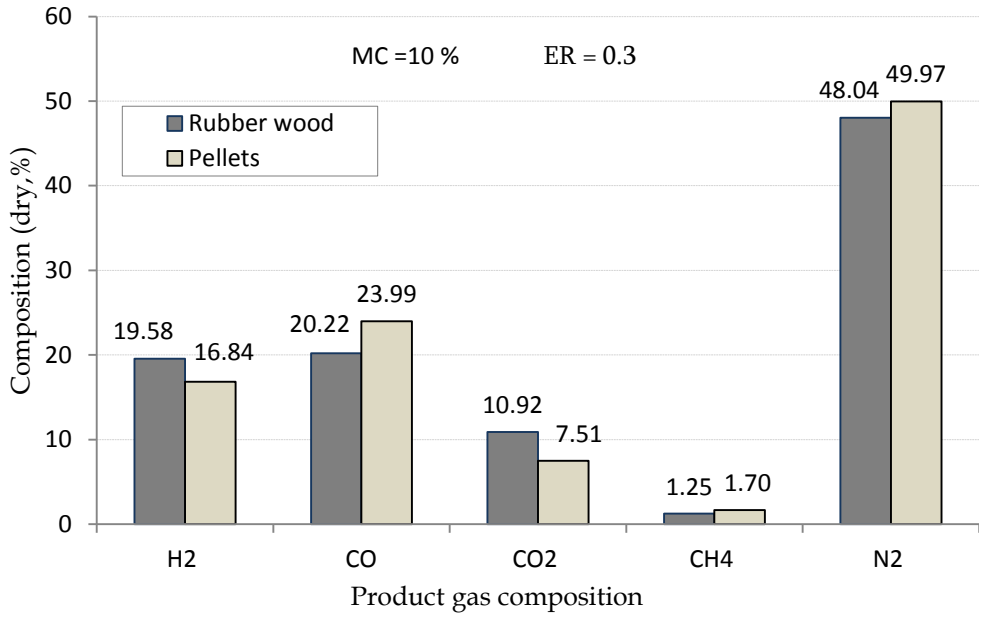

Figure 6.1 Final dry composition of product gas

Present model also possess capability to predict the maximum temperature that can be recorded from different zone. However, present model is incompetence to locate the position of pyrolysis zone. The maximum temperature that can be measured during gasification of rubber wood and pellets at 10% of moisture content and equivalence ratio of 0.3 are listed in Table 6.2.

Table 6.2 Maximum temperature achieved in each zone during simulation

	Temperature (K) (MC=10%, ER=0.3)		
Biomass	Pyrolysis	Oxidation	Reduction
Rubber wood	813.58	1375.54	906.09
Pellets	837.22	1422.69	908.44

When the dry gas composition is known, it is also possible to estimate the calorific heating value of the product gas, carbon conversion during the gasification process and cold gas efficiency.

The calorific heating value of the product gas depends on the composition of the gas and heating value of flammable gas such as H_2, CO and CH_4. The expression to calculate the heating value of gas mixture can be expressed as [46]:

$$HHV_{productgas} = HHV_{H_2} \times y_{H_2} + HHV_{CO} \times y_{CO} + HHV_{CH_4} \times y_{CH_4} (MJ/Nm^3) \quad (6.04)$$

The heating values of corresponding gas are mentioned in Appendix B3. With the aid of heating value, the cold gas efficiency (η_{cg}) of a gasifier can also be identified with the following relations [46]:

$$\eta_{cg} = \frac{HHV_{productgas}(MJ/Nm^3) \times \sum n_i(kmol/kg_{fuel}) \times 22.4(Nm^3/kmol)}{HHV_{biomass}(MJ/kg)} \quad (6.05)$$

where $\sum n_i(kmol/kg_{fuel})$ is the amount of product gas per kg of fuel (biomass) and can be estimated as[46]:

$$\sum n_i(kmol/kg_{fuel}) = \frac{N_{2\,wt.\%inair} \times A/F(kg_{air}/kg_{fuel})}{N_{2,\%productgas,d.b} \times M_{N_2}} \quad (6.06)$$

Finally, the carbon conversion at the calibrated reduction length of the gasifier is determined by the ratio of carbon on product gas to the carbon on the biomass received from ultimate analysis as weight basis, which can be numerically expressed as [47];

$$C_{conversion} = \frac{m_{f,CO(db)} + m_{f,CO_2(db)} + m_{f,CH_4(db)}}{m_{f,C,biomass(db)}} \times 100\% \quad (6.07)$$

On the basis of Eq. (6.04-6.07), the estimated HHV, cold gas efficiency and carbon conversion for rubber wood and pellets as feed are presented in table 6.3.

Table 6.3 HHV, η_{cg} efficiency and carbon conversion results (MC = 10%, ER = 0.3)

Biomass	HHV(MJ/Nm^3)	Cold gas efficiency (%)	Carbon conversion (%)
Rubber wood	5.54	68,62 %	83.00 %
pellets	5.72	71.57 %	82.46 %

7 Validation

The robustness, performance and utility of a mathematical model can be evaluated by comparing the results from the model with the experimental data achieved under similar process parameters. In the present model, the governing process parameters are moisture content and air to fuel ratio or equivalence ratio. Thus, the performance of present model is validated based on composition and temperature of different zone against the experimental data of Jayah et al.[34] with Rubber wood and Barrio et al. [35] with pellets under similar conditions. The experimental results are already mentioned in section 3.

7.1 Composition comparison

The composition of product gas is mainly determined by the biomass chemical composition, moisture content and equivalence ratio. Thus, on similar process parameter and similar biomass chemical composition, a robust mathematical model should yield identical results to that of experimental data.

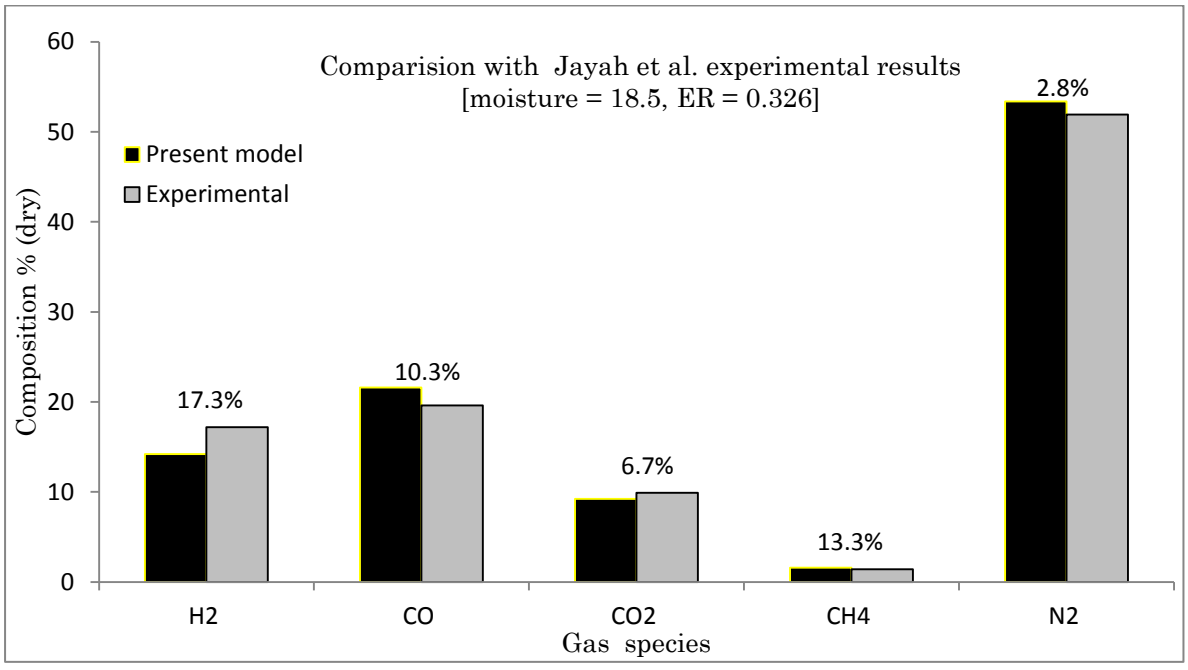

Figure 7.1 Composition comparisons with experimental data of Jayah el al.

Figure 7.1 shows the comparison of product gas compositions with the experimental data of Jayah et al. at 16% of moisture content and equivalence ratio of 0.35. The modeled data shows an absolute agreement with the

experimental data with average error for prediction <17%. The error is calculated with the help of Eq. (7.1).

$$\text{Error},_{\%} = \frac{\left|n_{i,model} - n_{i,experimental}\right|}{n_{i,experimental}} \times 100\% \tag{7.01}$$

$$\text{Accuracy},_{\%} = 100\% - \text{Error},_{\%}\,(\%) \tag{7.02}$$

Table 7.1 Comparison of product gas composition based on moisture content and A/F ratio (Jayah et al.)

Test	MC $\%_{w.b.}$	ER	H_2 (%)	CO (%)	CO_2(%)	CH_4(%)	N_2 (%)	$\text{Error},_{AVG}$
T1	18.5	0.326	17.20	19.60	9.90	1.40	51.90	
M			14.22	21.61	9.23	1.59	53.35	
Error,%			17.3 %	10.3 %	6.7 %	13.3 %	2.8 %	10.08 %
T2	16	0.353	18.30	20.20	9.70	1.10	50.70	
M			14.34	22.72	8.66	1.39	52.89	
Error,%			21.7 %	12.5 %	10.7 %	26.4 %	4.3 %	15.10 %
T3	14.7	0.380	17.20	19.40	9.70	1.10	52.60	
M			14.19	23.52	8.22	1.25	52.82	
Error,%			19.3 %	18.9 %	16.0 %	9.2 %	0.4 %	12.76 %
T4	16	0.315	17.00	18.40	10.60	1.30	52.70	
M			14.95	21.85	9.18	1.58	52.44	
Error,%			12.0 %	18.7 %	13.4 %	21.4 %	0.5 %	13.21 %
T5	15.2	0.340	13.20	19.70	10.80	1.30	55.00	
M			14.69	22.60	8.76	1.43	52.52	
Error,%			11.3 %	14.7 %	18.9 %	9.8 %	4.5 %	11.86 %
T6	14.7	0.299	15.50	19.10	11.40	1.10	52.90	
M			15.58	21.77	9.28	1.63	51.74	
Error,%			0.5 %	14.0 %	18.6 %	47.7 %	2.2 %	16.60 %
T7	13.8	0.327	12.70	22.10	10.50	1.30	53.40	
M			15.18	22.60	8.81	1.45	51.97	
Error,%			19.5 %	2.2 %	16.1 %	11.8 %	2.7 %	10.46 %

Furthermore, the validity of present model is tested under a wide range of process parameter similar to the experimental one and the results are

presented in table 7.1. The data sets reveal the preciseness of predictability of present model. Under various process parameter as mentioned in table 7.1, the average error of prediction ranges from 10% to maximum 17%. The error on prediction of H_2 varies from 0.5% to 19. Likewise, CO prediction error lies between 2.2% and 18.7%. CO_2 prediction error ranges from 6.7% to 18.1%. Similarly, the composition of CH_4 is predicted with an accuracy of 74.7% to 97.3%, whereas the accuracy of inert N_2 gas prediction is between 91% and 99.5%. The accuracy is calculated using Eq. (7.02).

To increase the reliability of present model, its validation is also tested against the experimental data measured by Barrio et al [35]. Figure 7.2 displays the comparison of product gas for modeled data vs. experimental data at moisture content of 6.38% and equivalence ratio of 0.282. The chart reveals a good agreement between the modeled data and the experimental data with an average accuracy of 91.44%.

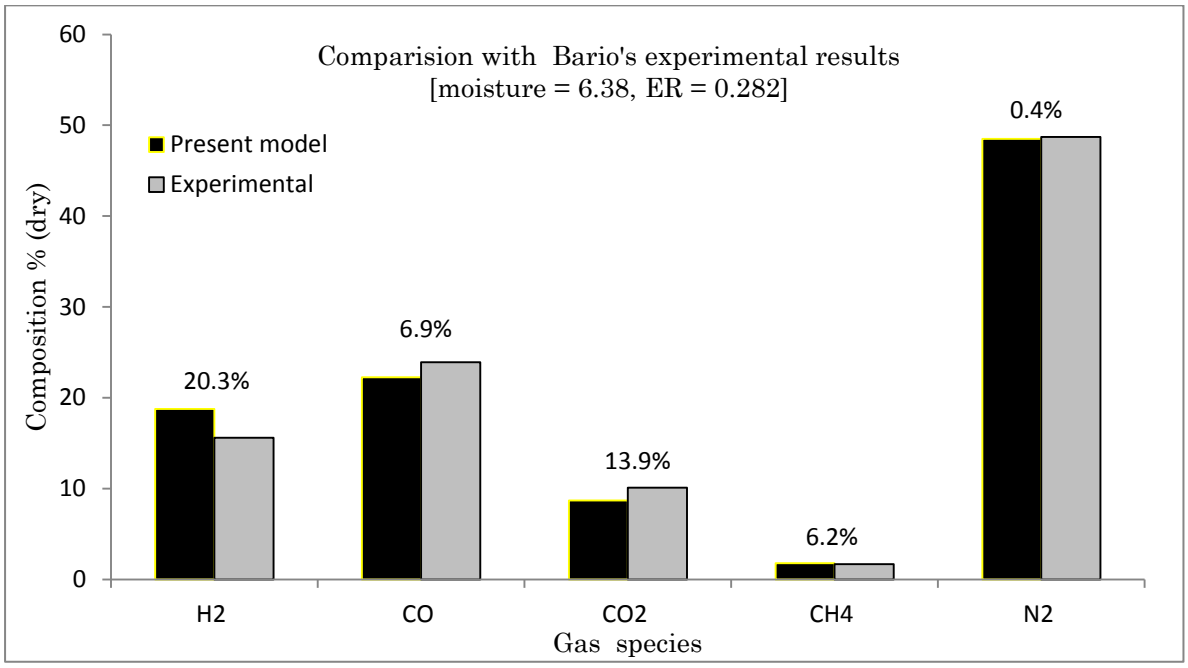

Figure 7.2 Composition comparisons with M. Barrio's experimental data

Moreover, the model is also validated under different process parameter value of moisture content and equivalence ratio. The moisture content is varied from 6.8% to 8%, while the equivalence ratio lies in the range of 0.247 to 0.29. The modeled results are listed in table 7.2 and compared against the experimental data obtained from analogous process parameter. Comparison with M. Barrio's experimental data also reveals a good agreement between the predicted value and the measured value of product gas composition.

Table 7.2 Comparison of product gas composition based on moisture content and A/F ratio (Barrio et al.)

Test	MC $\%_{w.b.}$	ER	H_2 (%)	CO (%)	CO_2 (%)	CH_4 (%)	N_2 (%)	$Error_{AVG}$
#8b	7.25	0.261	16.8	25.8	9.1	1.5	46.8	
M			19.17	21.44	9.12	2.00	48.28	
Error,%			14.1 %	16.9 %	0.2 %	33.0 %	3.2 %	13.48 %
#9	6.9	0.290	15.5	25.3	9.3	1.5	47.3	
M			18.47	22.38	8.61	1.76	48.78	
Error,%			19.1 %	11.5 %	7.4 %	17.6 %	3.1 %	11.78 %
#12	7.02	0.287	16.4	25.2	9.4	1.5	47.5	
M			18.55	22.23	8.69	1.80	48.73	
Error,%			13.1 %	11.8 %	7.6 %	19.9 %	2.6 %	10.99 %
#13a	6.38	0.282	15.6	23.9	10.1	1.7	48.7	
M			18.76	22.24	8.69	1.81	48.50	
Error,%			20.3 %	6.9 %	13.9 %	6.2 %	0.4 %	9.56 %
#13b	8	0.259	17.2	26.4	8.8	1.4	46.3	
M			19.13	21.18	9.25	2.05	48.39	
Error,%			11.2 %	19.8 %	5.1 %	46.4 %	4.5 %	17.41 %
#13c	7.58	0.247	16.4	25.2	9.4	1.5	47.5	
M			20.08	19.94	9.88	2.38	47.71	
Error,%			22.5 %	20.9 %	5.1 %	59.0 %	0.4 %	21.58 %
#14	6.67	0.278	16.4	25.3	9.4	1.5	47.4	
M			20.16	20.04	9.83	2.36	47.61	
Error,%			22.9 %	20.8 %	4.5 %	57.3 %	0.4 %	21.20 %

7.2 Temperature comparison

Temperature of gasifier, alike gas composition, is also governed by the biomass chemical compositions, moisture content and equivalence ratio. Thus, the validity of present model on prediction of temperature is tested against the temperature recorded during the experimental investigation performed by Jayah et al. [34].

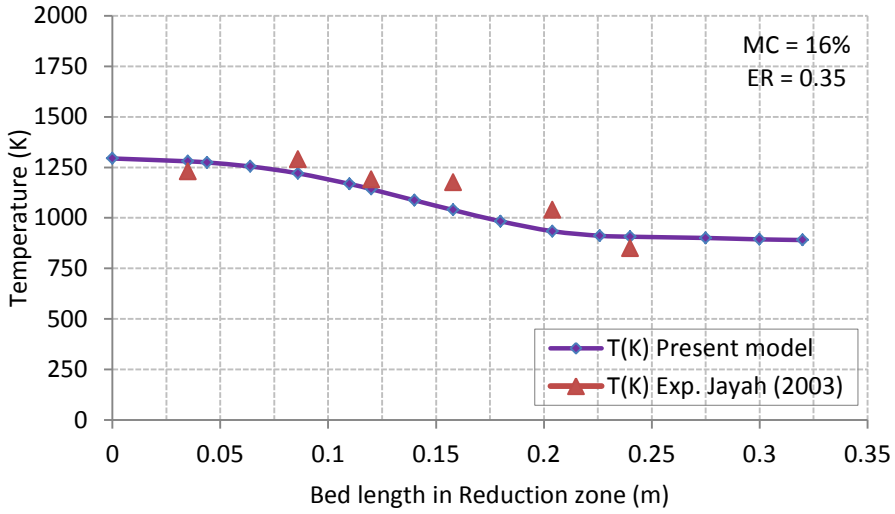

Figure 7.3 Comparison of temperature along length of reduction zone

Figure 7.3 displays the temperature measured (experimental) along the reduction zone length and the predicted temperature at moisture content of 16% and equivalence ratio of 0.35. The prediction shows a good agreement at the starting and end of reduction zone between the predicted value and the experimentally measured value.

Temperature profile comparison with Barrio et al. experimental data is not performed since present model is partly based on equilibrium model and equilibrium models does not incorporate any gasifier design parameters. However, the finite kinetic model have been adapted for reduction sub-model, it is not robust to identify the location of pyrolysis and oxidation zone in the gasifier.

7.3 Heating value and cold gas efficiency comparison

Heating value received from product gas and cold gas efficiency are important aspects of a gasification process. It is also worthwhile to validate the present model based on the lower heating value (LHV) and cold gas efficiency (η_{cg}) measured during experimental investigation. Table 7.3 shows the comparison of LHV and cold gas efficiency between the experimental value from M. Barrio's investigation and predicted value.

The average accuracy in prediction of LHV of the product gas is about 97.5%, while the cold gas efficiency has been predicted with an average error of 1.8%.

Table 7.3 Comparison of lower heating value and cold gas efficiency

Experiment Number		#8b	#9	#12	#13a	#13b	#13c	#14
LHV	Exp.	5.4	5.6	5.5	5.3	5.7	5.5	5.5
(MJ/Nm3)	Model	5.63	5.57	5.57	5.60	5.61	5.65	5.60
	Error,%	4.3 %	0.5 %	1.3 %	5.7 %	1.6 %	2.7 %	1.8 %
η_{cg} (%)	Exp.	60	64	64	60	59	55	62
	Model	59.25	64.17	63.46	63.22	58.34	56.8	62.29
	Error,%	1.3 %	0.3 %	0.8 %	5.4 %	1.1 %	3.3 %	0.5 %

Ultimately, the validation of present model exhibits a reliable and accurate prediction of product gas composition, temperature of gasifier, heating value of product gas and cold gas efficiency of gasifier. Thus, the present models may be employed to identify the optimal operational parameters.

8 Sensitivity analysis

The present three zone model that has been validated with published experimental results with considerable accuracy. Then, it is used for investigating the influence of moisture content and equivalence ratio on product gas composition of each zone, temperature, carbon conversion and cold gas efficiency for Rubber wood as a feed stock. One advantage of robust model is its suitability to check the gasifier's performance at extreme limits of operating parameters, which might be risky and uneconomical from experimental aspects.

8.1 Influence of moisture content

The moisture content of a biomass has been varied from 0% to 30% at equivalence ratio of 0.3, and its effect on the composition of gas at each zone is studied. The results of moisture variation can be summarized as:

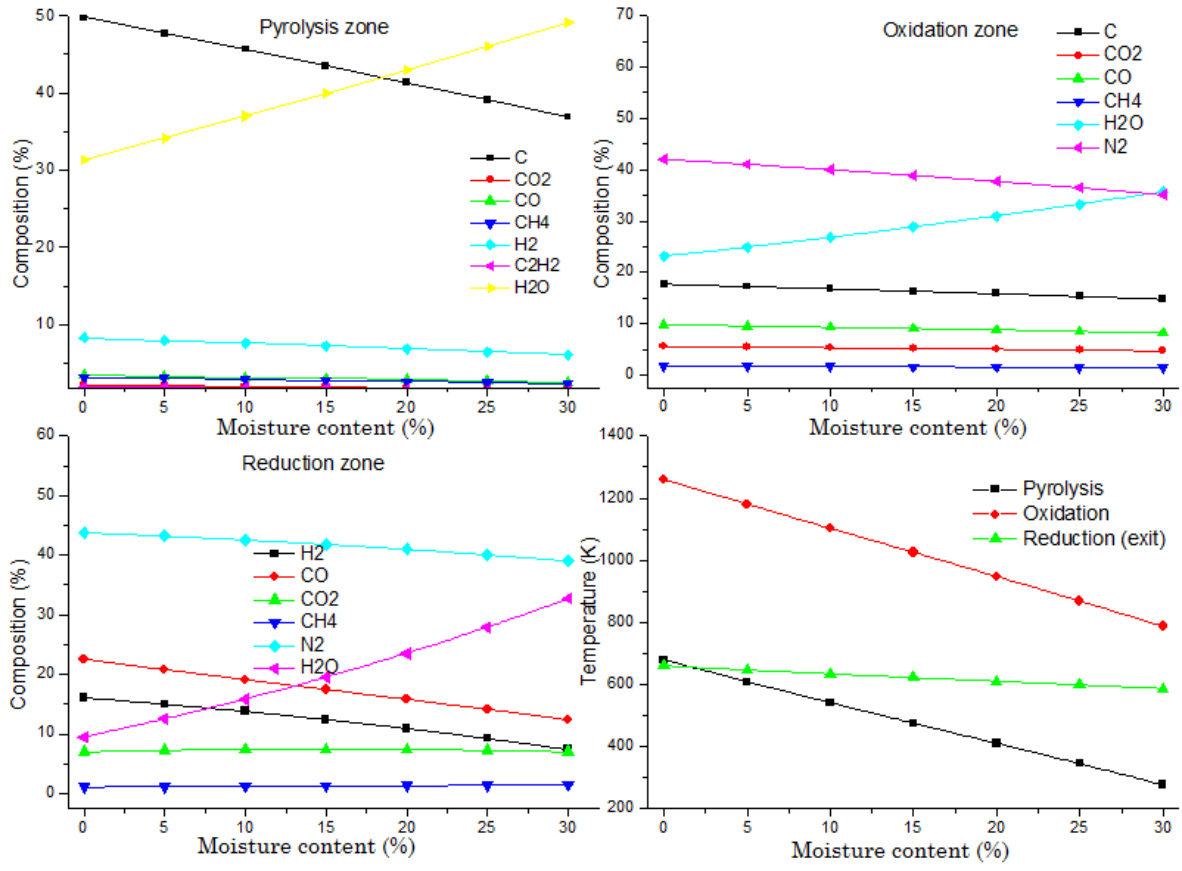

Figure 8.1 Effect of moisture content on composition of chemical species and temperature profile in each zone

The present three zone model facilitates to examine the change in composition of each chemical species involved in gasification at different zone. Figure 8.1 displays the effect of moisture on concentration of C_{char}, CO, CO_2, H_2, CH_4, C_2H_2, H_2O and N_2 at pyrolysis, oxidation and reduction zone respectively. However, the effect of moisture content on final dry composition of product gas is meaningful to assess. So, the effect of moisture content on dry composition of products gas is presented in figure 8.2. Based on the model assessment, dry concentration of flammable gas such as H_2 and CO decreases as the moisture in the feed increases, whereas slight increase in CH_4 concentration has been predicted with increase in moisture amount. The concentration of diluting gas like N_2 and CO_2 are found to be increasing with high moisture content. Since the heating value of product gas is mainly due to the calorific value of H_2, CO and CH_4, it can be concluded that lower moisture amount are preferred in the biomass in order to achieve higher concentration of corresponding gas and heating value. The moisture present in the biomass also affects the temperature of the gasifier. The study reveals decrease in temperature of each zone, which can be supported by the fact that higher amount of heat energy is required to evaporate the moisture from the biomass. This in turn results to decrease in the temperature at each zone.

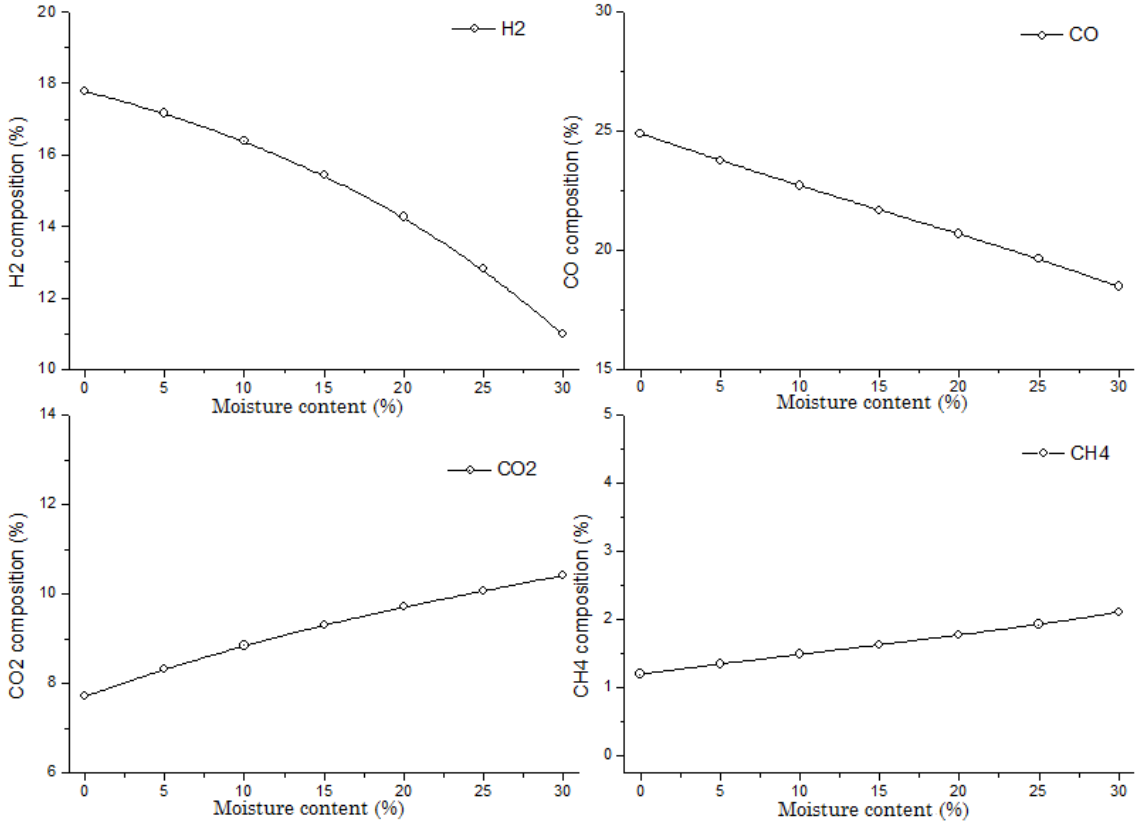

Figure 8.2 Effect of moisture content on dry gas composition

Figure 8.3 depicts the influence of moisture content on N_2 composition, heating value of product gas, overall carbon conversion of the gasification process and cold gas efficiency of the gasification system. N_2 composition of dry product gas increases with increase in moisture content. Likewise, both LHV and HHV, carbon conversion, cold gas efficiency decreases with increment in amount of moisture content. The decrease in heating values of product gas is most likely due to dilution by N_2 and H_2O.

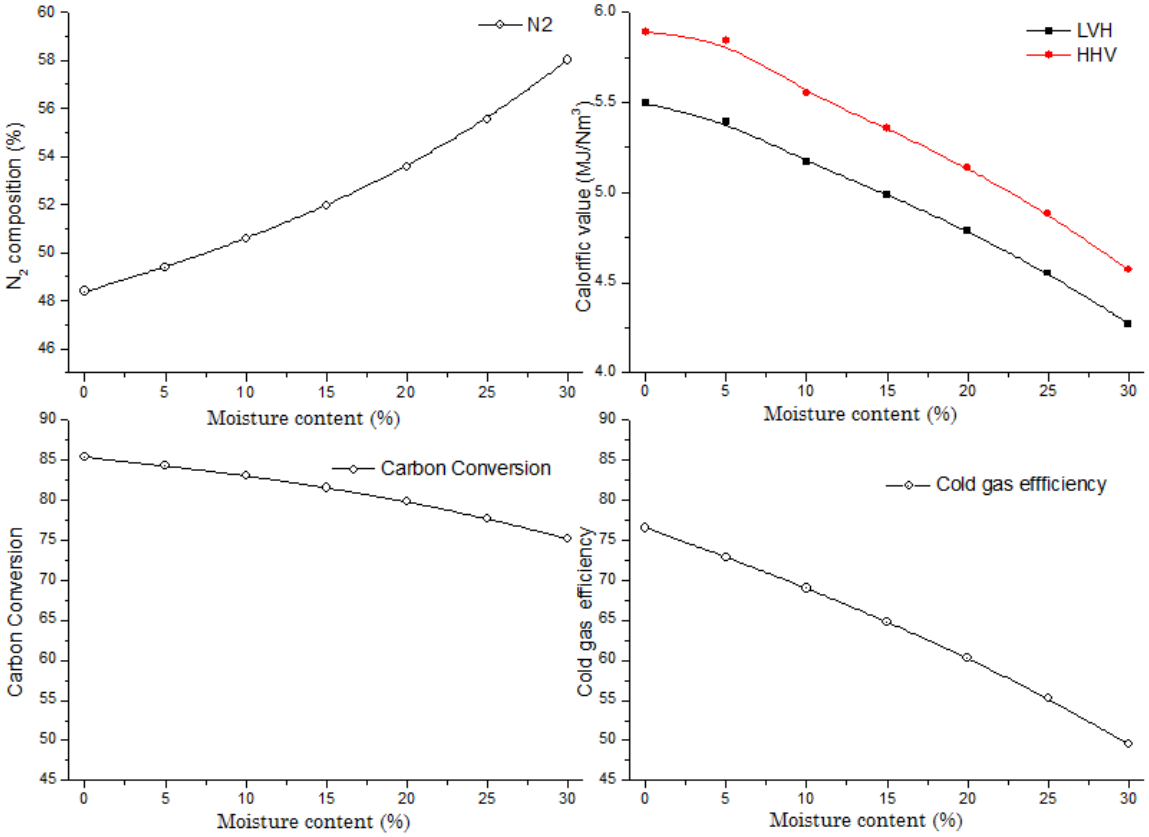

Figure 8.3 Effect of moisture content on heating value, cold gas efficiency and carbon conversion

Thus, lower moisture contents are identified as optimal operational parameters in downdraft biomass gasification process.

8.2 Influence of equivalence ratio

Equivalence ratio (λ) is also one of the operational parameters that have significant competence to determine the fate of composition of chemical species involved in gasification. The typical equivalence ratio for a gasification process is found to be in the range of 0.268-0.43 [48]. However, the behavior of any biomass gasifier can be tested beyond the typical range of equivalence ratio

without any risk and hazards to the gasification unit with the aid of present model.

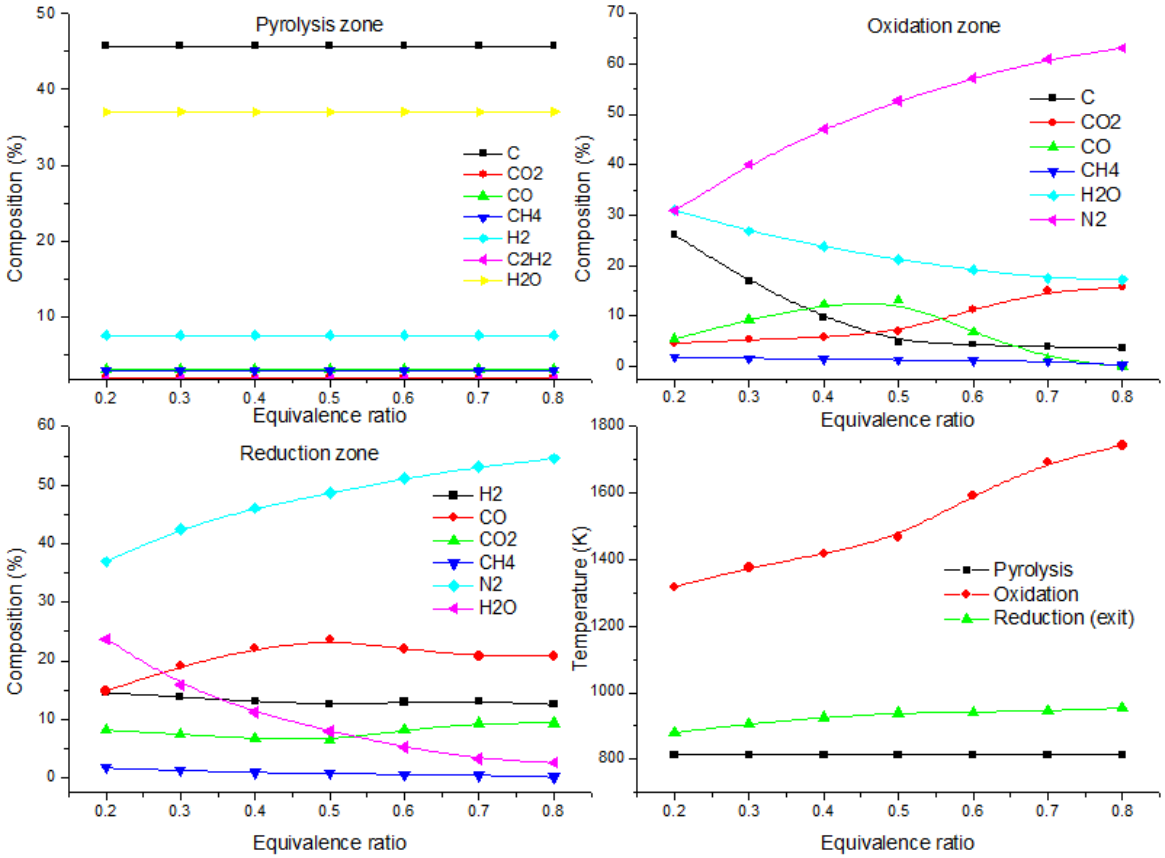

Figure 8.4 Effect of equivalence ratio on composition of chemical species and temperature profile in each zone

Figure 8.4 depicts the effect of equivalence ratio on the composition of various chemical species involved in the respective zone. There is no effect of equivalence ratio increment on the composition of pyrolysis zone because it does not incorporate any mechanism with supplied air. The increment in equivalence ratio indicates supply of more amount of air in the system, which in turn increase the concentration of N_2 in both oxidation and reduction zone, while change in concentration of other chemical species are also apparent in figure 8.4. The influence of equivalence ratio on dry gas composition of product gas is displayed in figure 8.5. Higher equivalence ratio results in increase in concentration of N_2, as more air is supplied. CO composition is found to be increasing up to $\lambda = 0.45$ and then decreases with higher equivalence ratio and CO_2 composition decreases up to $\lambda = 0.45$ and then increase with increase in equivalence ratio. Meanwhile, the composition of H_2, and CH_4 decreases with increase in equivalence ratio. However, such prediction does not seem to be valid when compared to experimental results as elaborated in [48].

The influence of equivalence ratio is also studied on the temperature of different zone of the gasifier, and the results are shown in figure 8.4. The results indicate increase in temperature of oxidation and reduction zone, while the temperature of pyrolysis zone seems to be decreasing. The insignificant increment in oxidation and reduction temperature along with decrement in pyrolysis temperature is because of heat loss from each zone, as heat loss has been estimated to be 10% of the product of equivalence ratio and heating value of the biomass.

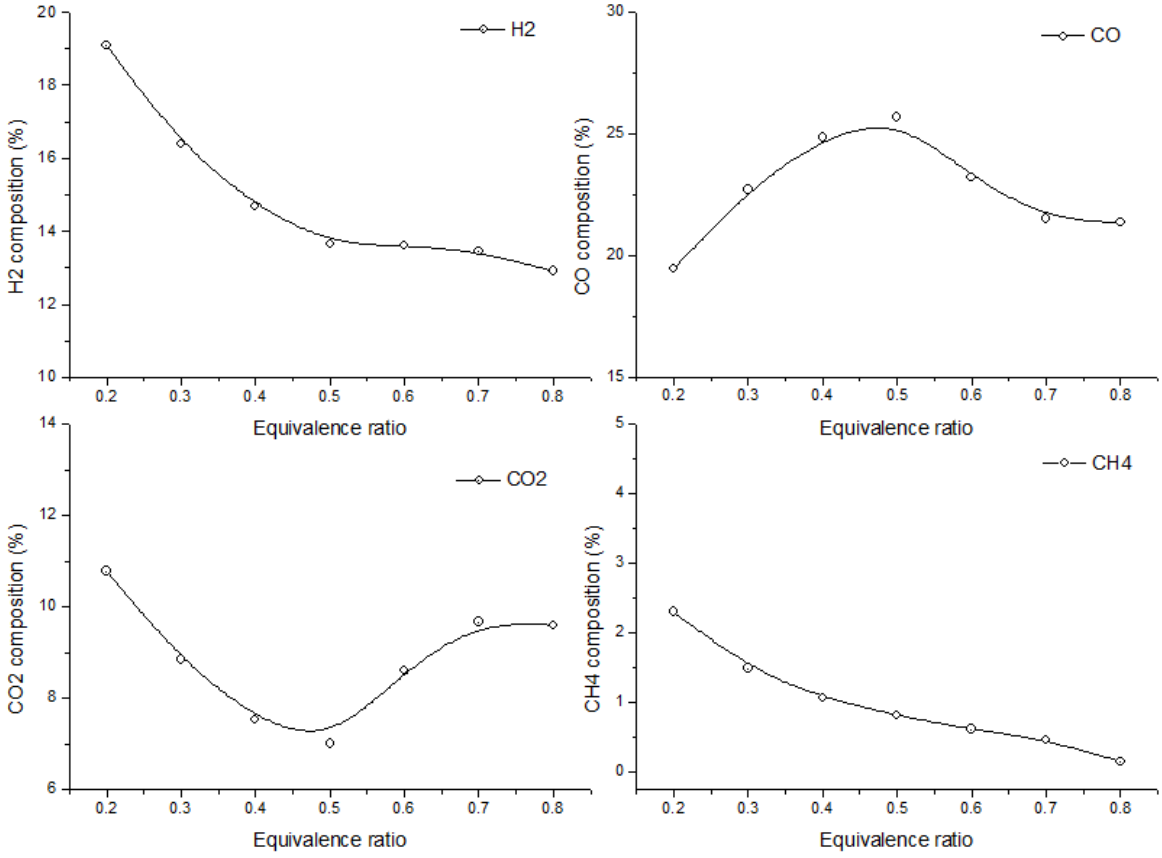

Figure 8.5 Effect of equivalence ratio on dry gas composition

Figure 8.6 represents the influence of equivalence ratio on carbon conversion and cold gas efficiency. The results suggest that there is decrement in carbon conversion and cold gas efficiency with increase in equivalence ratio.

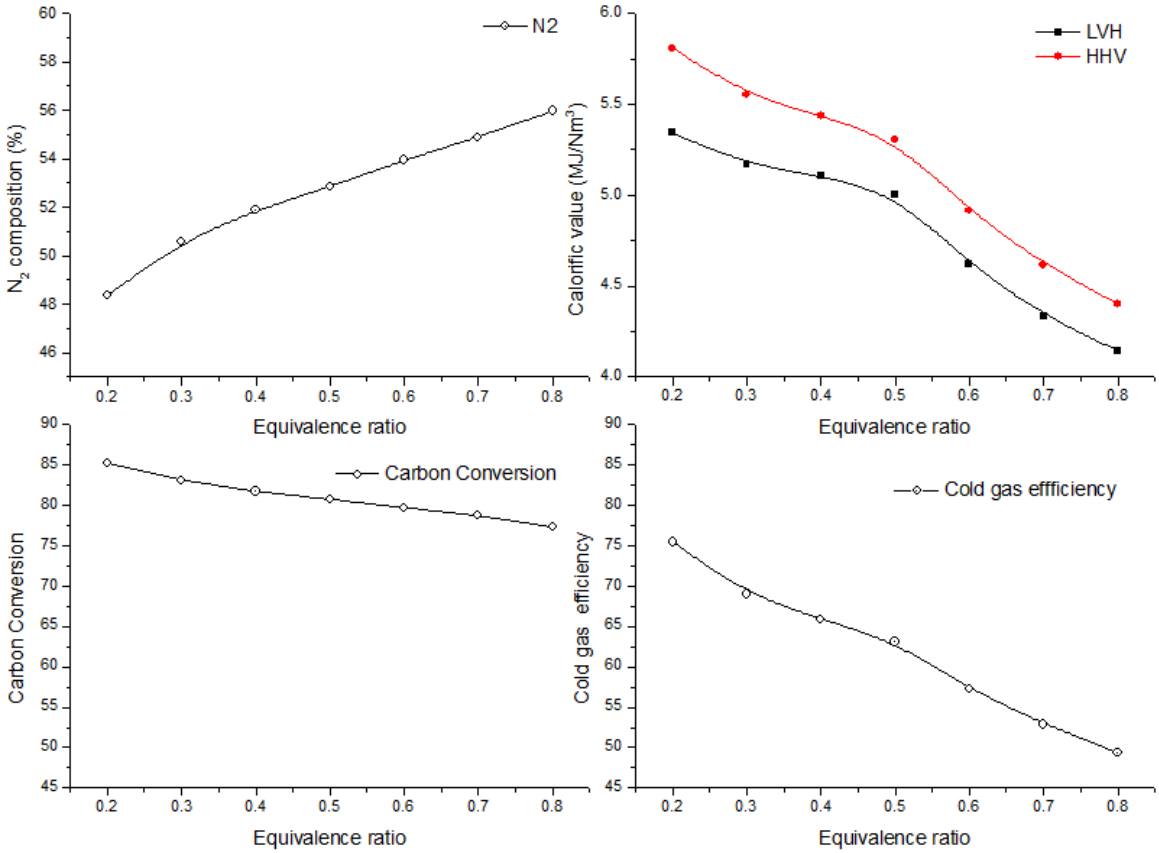

Figure 8.6 Effect of moisture content on N_2 composition, heating value, cold gas efficiency and carbon conversion

The sensitivity analysis based on equivalence ratio seems to have some discrepancy with the experimental results such as LHV over 4MJ/Nm^3 at λ = 0.8 is not possible due to dilution by the air nitrogen. Thus, further development of present model is required to establish a robust and competent mathematical model.

9 Limitation and Uncertainty analysis

A robust mathematical model may have several advantages, but some limitations are inevitable. Present model is established based on thermodynamic stoichiometric equilibrium approach for pyrolysis and reduction zone, while reduction zone is modeled based on finite kinetic approach. Thus, both modeling approach have several limitations, which are summarized as following:

- The equilibrium model is restraint from the design and operational parameter such as length of gasifier, pressure inside the gasifier, and hydrodynamics of the system. Thus, present model is incompetent of determining the exact location of pyrolysis and oxidation zone.
- Finite kinetic modeling approach for reduction zone is also incapable of determining the hydrodynamics of gasifier and residence to time for each gaseous species involved in gasification.
- Utility of present model is limited only to wood based biomass as feed..
- Present model does not account for formation of tar, higher hydrocarbon during gasification process and phase change of thus formed higher hydrocarbons.
- The reduction zone does not reveal the actual reactivity of char as it is represented by the char reactivity factor.

Besides the limitation, present modeling also reflects some uncertainty in prediction of composition of product gas and temperature of the gasifier. Such uncertainties in present model are as consequence of following reasons:

- The equilibrium models are based on empirical assumptions, and create immense uncertainties on the reliability of the whole model.
- The assumptions implicated in pyrolysis and oxidation zones may create discrepancies against the experimental results and may induce the magnitude of uncertainties.
- The uncertainty of relating or scaling the dimension of gasifier to the dimension of mathematical model is one of the crucial aspects in present modeling work. This results in uncertainty in selection of proper length for various zone especially reduction zone length.
- Different correlation used for numerical calculations also ascent the uncertainty of present model to some extent.

10 Conclusions

The objective of present thesis work is to study different aspects of modeling relating to downdraft gasifier. In addition, the objective also includes revision of finite kinetic model for reduction zone of downdraft gasification process, formulating separate sub-models for pyrolysis and oxidation zone, then integrating these sub-model to establish a revised version of mathematical model. Thus, a mathematical model has been formulated for the simulation of behavior of fixed bed downdraft gasifier. Separate sub-model for pyrolysis, oxidation has been established based on equilibrium approach and successfully integrated with revised kinetic model for reduction zone. An exponential variation of char reactivity factor (C_{RF}) has been considered along the gasifier length in order to incorporate the char reactivity in the reduction zone. The composition of product gas and temperature of different zone have been predicted precisely in the present model. EXCEL has been used as computational tool for present three zone model.

The model has been validated against the experimental data published in the open literatures. Data such as final dry gas composition, gasifier temperature, heating value of product gas and cold gas efficiency are obtained from the experimental investigation. Then, the results of present model have been compared with the experimental data. The compositions of the product gas have been predicted with an accuracy of ~90% in average. Meanwhile, the temperature profile along the gasifier has also been predicted with reasonable precision. Similarly, the comparison of heating value and cold gas efficiency between modeled value and experimental value also reveals remarkable agreements.

A parametric investigation has been performed at different moisture content and equivalence ratio. Increase in moisture content results in decrement of flammable gas like CO and H_2, which in turn decreases the heating value of the product gas. Decrement in temperature of pyrolysis, oxidation and reduction zone has been noticed as moisture content increases. This is because more heat is consumed to evaporate the water from the biomass resulting decrease in the gasifier efficiency. Thus, lower moisture content in the biomass is advocated for obtaining high gas yield with higher efficiency. Moreover, decrease in concentrations of H_2, CO and CH_4, while increments of CO_2 concentration have been observed with increasing equivalence ratio. Lower heating value of >4MJ/Nm^3 has been observed at equivalence ratio of 0.8, which has provoked the uncertainties of model in prediction of gas composition at higher equivalence ratio.

Finally, the three zone equilibrium and finite kinetic model of downdraft gasifier displays a perceptible validation and the good agreement between the modeled and measured value. However, there are certain limitations and uncertainties in present model, which needs to be further developed and improved with addition of extra features and employing different computational approaches.

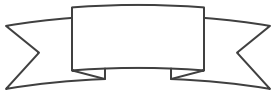

11Appendices

Appendix A Calculation of Biomass properties

A1. Estimation of heat of formation of biomass

Hess's law is employed to estimate the heat of formation of biomass. The generic reaction for formation of biomass may be modeled as:

$$C + 0.76H_2 + 0.31O_2 \rightarrow CH_{1.53}O_{0.626}$$ (Rubber wood)

As the Hess's law states that *ΔH for a reaction can be found indirectly by summing ΔH values for any set of reactions which sum to the desired reaction.* Then, the modeled reaction can be approached by following reactions. Reaction A represents the oxidation of carbon, reaction B represents oxidation of hydrogen and reaction C represents oxidation of the biomass. The heat of reaction of these reactions can be retrieved from the Appendix B, as reaction A accounts for heat of formation of CO2, reaction B accounts for heat of formation of water and reaction C accounts for higher heating value of the biomass.

Reactions	ΔH_f (kJ/kmol)
A) $C + O_2 \rightarrow CO_2$	-393509
B) $0.765H_2 + 0.3825O_2 \rightarrow 0.765H_2O$	-185078.1322
C) $CH_{1.53}O_{0.62} + 1.072O_2 \rightarrow CO_2 + 0.765 H_2O$	-488733.0345
D) $C + 0.76H_2 + 0.31O_2 \rightarrow CH_{1.53}O_{0.62}$	**-89854.09774**

Finally, the heat of formation of biomass can be estimated as; D = A+B-C.

Thus, the heat of formation of rubber wood is estimated as -89854.0977 kJ/kmol.

Similar approach is made to estimate the heat of formation of biomass in [7].

Appendix B Constant Parameter

B1. Thermodynamic property table [10]

			Gibbs free energy	Heat of formation	Heat Capacity Constants(A, B, C, D)				
Species	Phase	Molar mass (g/mol)	$g°_f$ at 298K (kJ/kmol)	$h°_f$ at 298K (kJ/kmol)	Tmax	A	10E3*B	10E6*C	10E-5D
H_2O	g	18.0153	-228572	-241818	2000	3.47	1.45	-	0.121
H_2O	l	18.0153	-237129	-285830	-	-	-	-	-
CO_2	g	44.01	-394359	-393509	2000	5.457	1.047	-	-1.157
CO	g	28.01	-137169	-110525	2500	3.376	0.557	-	-0.031
CH_4	g	16.042	-50460	-74520	1500	1.702	9.081	-2.164	-
H_2	g	2.0159	0	0	3000	3.249	0.422	-	0.083
O_2	g	31.9998	0	0	-	-	-	-	-
N_2	g	28.0134	0	0	2000	3.28	0.593	-	0.04
C	s	12.0107	0	0	2000	1.771	0.771	-	-0.867

The above mentioned heat capacity constants are for estimation of c_p by correlation;

$$c_p = R\left(A + BT_{am} + \frac{C}{3}\left(4T_{am}^2 - T_{atm}T_P\right) + \frac{D}{T_{atm}T_P} \right)$$

B2. Thermodynamic property table [49]

			Gibbs free energy	Heat of formation	Heat Capacity Constants (a, b, c, d)				
Species	Phase	Molar mass (g/mol)	$g°_f$ at 298K (kJ/kmol)	$h°_f$ at 298K (kJ/kmol)	Tmax	a	b	c	d
H_2O	g	18.0153	-228572	-241818	1800	32.34	1.92E-03	1.06E-05	-3.60E-09
H_2O	l	18.0153	-237129	-285830					
CO_2	g	44.01	-394359	-393509	1800	22.26	5.98E-02	-3.50E-05	7.47E-09
CO	g	28.01	-137169	-110525	1800	28.16	1.68E-03	5.37E-06	-2.22E-09
CH_4	g	16.042	-50460	-74520	1500	19.89	5.02E-02	1.27E-05	-1.10E-08
H_2	g	2.0159	0	0	1800	29.11	-1.92E-03	4.00E-06	-8.70E-10
O_2	g	31.9998	0	0	1800	25.48	1.52E-02	-7.16E-06	1.31E-09
N_2	g	28.0134	0	0	1800	28.9	-1.57E-03	8.08E-06	-2.87E-09
C_2H_2	g	26.038	209170	226730	1500	21.8	9.214E-02	-6.527E-05	1.821E-08

The above mentioned heat capacity constants are for calculation of c_p by correlation;

$$c_p = a + bT + cT^2 + dT^3$$

B3. Standard heating value of product gas [50]

Gases	H_2	CO	CO_2	CH_4	N_2	C_2H_2
HHV (MJ/Nm3)	12.74	12.63	0	39.82	0	58.06
LHV (MJ/Nm3)	10.78	12.63	0	35.88	0	56.07

Appendix C Formulation of mathematical model

C1. Formulation of pyrolysis model

From first postulate, 4/5 of fuel oxygen is associated with fuel '*h*' in the form of H_2O, which can be formulated as:

$\left(\frac{4}{5}\times o\right)=0.5008$, which implies; 0.5008 mol of O reacts with H to form H_2O i.e.,

$$0.5008O + n_h H \rightarrow n_{H_2O} H_2O \tag{C1.01}$$

From the stoichiometric equation for reaction between O and H to form H_2O, we get;

$$O + 2H \rightarrow H_2O \tag{C1.02}$$

The stoichiometric equation reveals that 1 mole of O reacts with 2 mol of H to produce 1 mole of H_2O. Thus, for Eq. (C1.01)0.5008 mol of O should react with 1.001 mol of H to form 0.5008 mol of H_2O.

Amount of fuel *h* consumed (n_h) = 1.001 mole

Amount of H_2O released (n_{H_2O}) = 0.5008 mole

Total amount of H_2O in pyrolysis zone (n_{p,H_2O}) = w + n_{H_2O} =0.750 mole

The second postulate depict that 1/5 of the fuel oxygen is associated with the fuel carbon and released as CO and CO_2.

$\left(\frac{1}{5}\times o\right)=0.125$; implies that 0.125 mol of O reacts with C from fuel and produces CO and CO_2 i.e.,

$$0.125O + n_C C \rightarrow n_{p,CO_2} CO_2 + n_{p,CO} CO \tag{C1.03}$$

From oxygen balance of Eq. (5.16);

$$0.125 \rightarrow 2n_{p,CO_2} + n_{p,CO} \tag{C1.04}$$

The third postulate depict that the ratio of mol of CO and CO_2 is inversely related with their molecular mass i.e.,

$$\frac{n_{p,CO}}{n_{p,CO_2}} = \frac{44}{28} \tag{C1.05}$$

Computation of Eq. (C1.04-C1.05) results to concentration of CO and CO_2 formed.

Thus, $n_{p,CO} = 0.0548$ and $n_{p,CO_2} = 0.0349$

Observation of stoichiometric reaction between C and O as mentioned in Eq. (C1.06) indicates that 3 mol of O reacts with 2 mol of C.

$$3O + 2C \rightarrow CO_2 + CO \tag{C1.06}$$

Finally, it can be concluded for Eq. (C1.03) that 0.125 mol of O reacts with $\frac{2}{3} \times 0.125 = 0.0834$ mol of C.

The fourth postulate states 50% of available hydrogen in the fuel is released as H_2. It has been observed that 1.001 mole of fuel h has been consumed during H_2O formation. Thus, amount of 'fuel h' remaining can be estimated as:

$$h_r = h - n_h = 1.53 - 1.001 = 0.529 mole$$

Now, 50% of h_r (0.2645) is released as H_2. So, no. of mol of H_2 released can be calculated as

$$n_{p,H_2} = \frac{50\% \times h_r}{2} = 0.1322$$

Fifth postulate depict that remaining 50% of fuel h is released in the form of CH_4 and C_2H_2 i.e.,

$$50\% \times h_r H + n_C C = n_{p,CH_4} CH_4 + n_{p,C_2H_2} C_2H_2 \tag{C1.07}$$

From hydrogen balance of Eq. (5.16), we get;

$$50\% \times h_r = 4n_{p,CH_4} + 2n_{p,C_2H_2} \tag{C1.08}$$

The last postulate describes that ratio of mol of CH_4 and C_2H_2 is also inversely related with their molecular mass, i.e.,

$$\frac{n_{p,CH_4}}{n_{p,C_2H_2}} = \frac{26}{16} \tag{C1.09}$$

Solution of Eq. (C1.08-C1.09) gives the value of n_{p,CH_4} = 0.0505 mole and n_{p,C_2H_2} = 0.0311 mol.

Finally, the values of n_{p,CO_2}, $n_{p,CO}$, n_{p,CH_4}, n_{p,H_2}, n_{p,C_2H_2} & n_{p,H_2O} have been estimated through stoichiometric approach. Substituting values of n_{p,CO_2}, $n_{p,CO}$, n_{p,CH_4}, n_{p,C_2H_2} in Eq. (5.15) (carbon balance equation), we get; $n_{p,C}$ = 0.797 mol.

The estimation of pyrolysis products can also be approached by other computational techniques and the values may differ when using different correlations and different operational parameters.

C2. **Formulation of oxidation sub-model**

Based on the proposed assumptions, mathematical formulation of stoichiometric equation is very essential to achieve the objective of modeling i.e., to imitate artificially the actual chemical behavior under provided condition.

The first postulate depict that hydrogen formed during pyrolysis of biomass is fully oxidized to H_2O. i.e.,

$$0.132H_2 + n_{O_2}O_2 \rightarrow n_{H_2O}H_2O \qquad \text{(C2.01)}$$

The stoichiometric equation for reaction between O and H to form H_2O, indicates that 1 mol of H_2 reacts with 1/2 mol of O_2 to produce 1 mol of H_2O. Thus, 0.132 mol of H_2 should reacts with 0.066 mol of O_2 to yield 0.132 mol of H_2O.

Amount of H_2O produced = 0.132 mol

Amount of O_2 consumed = 0.066 mol

Based on second postulate, the balanced O_2 oxidizes C_2H_2 and yields CO_2 and H_2O i.e.,

$$0.031C_2H_2 + n_{O_2}O_2 \rightarrow n_{CO_2}CO_2 + n_{H_20}H_20 \qquad \text{(C2.02)}$$

$$2C_2H_2 + 5O_2 \rightarrow 4CO_2 + 2H_20 \qquad \text{(C2.02)}$$

The stoichiometric reaction between C_2H_2 and O_2 reveals that 2 mol of ethylene reacts with 5 mol of oxygen to produce 4 mol of carbon dioxide and 2 mol of water. Thus, it is also relevant to report that 0.031 mol of C_2H_2 reacts with $\frac{5}{2}\times 0.031 = 0{,}0775$ mol of O_2 to produce $\frac{4}{2}\times 0.031 = 0{,}062$ mol of CO_2 and $\frac{2}{2}\times 0.031 = 0{,}031$ mol of H_2O.

From Eq. (5.13), the amount of O_2 injected to the system is 0.348 mol. Thus, remaining O_2 in oxidation zone is estimated as;

$O_{2,rem} = (a - O_{2,\text{consumed by H2}} - O_{2,\text{consumed by C2H2}})$

$= 0.397 - 0.066 - 0.0775 = 0.2535$ mol

Third postulate narrates that remaining oxygen is consumed in char oxidation to produce CO and CO_2 i.e.,

$$0.2535O + n_C C \rightarrow n_{ox,CO_2} CO_2 + n_{ox,CO} CO \tag{C2.03}$$

Analyzing the oxygen elemental balance of Eq. (C2.03), we get;

$$0.2535 \rightarrow 2n_{ox,CO_2} + n_{ox,CO} \tag{C2.04}$$

According to fourth postulate, the ratio of formation of CO and CO_2 is inversely proportional to the exothermicity of their reactions. i.e.,

$$\frac{n_{ox,CO}}{n_{oxCO_2}} = 3.5606 \tag{C2.05}$$

Solving Eq. (4.33-4.34) we get the value of $n_{ox,CO} = 0.404$ and $n_{oxCO_2} = 0.113$ simultaneously.

Fifth postulate states, CO, CO_2 and H_2O formed during the pyrolysis are assumed to add up to the composition of oxidation zone. Thus,

$$n_{ox,CO} = 0.055 + 0.404 = 0.459 mole$$

$$n_{ox,CO_2} = 0.035 + 0.113 = 0.148 mole$$

$$n_{ox,H_2O} = 0.132 + 0.031 + 0.750 = 0.913 mole$$

The sixth postulate says CH_4 is carried forward to the reduction zone. So,

$$n_{ox,CH_4} = 0.050 mole$$

The last postulate describes that N_2 present in air does not participate in chemical reaction. Thus,

$$n_{ox,N_2} = a \times 3.76 = 1.493 moles$$

Finally, substituting known value in Eq. (5.22) results the value of char left in oxidation zone i.e., $n_{ox,C} = 0.341 moles$.

Thus mentioned computation approach reflects one solution, however several other approaches may be utilized to estimate the final composition of oxidation product.

C3. **Formulation of reduction sub-model**

The reduction zone is partitioned into n number of compartments of length $\Delta z = 0.001$ mm. The gas composition, temperature for first section is taken from the output oxidation sub-model. The initial pressure at the initial compartment of reduction zone is assumed to be 1.005 atm (10050 Pa) as the pressure at the outlet remains above atmospheric pressure [27]. The velocity of gas inside the gasifier is dependent to mass and size of biomass particles and temperature of corresponding phase. The variation in the gas velocity lies between 0.4 m/s to 1.2 m/s [51]. Thus, the initial velocity of gaseous species in reduction zone is assumed to be 0.5 m/s. As the reduction zone is partitioned into n number of Δz section, the parameters for n^{th} section are determined on the basis of $(n-1)^{th}$ section. Thus, the change in molar concentration of each gaseous species at consecutive n^{th} section can be modeled by:

$$\frac{dn_x}{dz} = \frac{1}{v}\left(R_x - n_x \frac{dv}{dz}\right)$$

Modifying the above equation for estimating the gas composition at n^{th} section results to:

$$n_i^n = n_i^{n-1} + \left[\frac{1}{v_{n-1}}\left(R_i^{n-1} - n_i^{n-1}\frac{v_n - v_{n-1}}{\Delta z}\right)\right] \times \Delta z \qquad \text{(C3.01)}$$

As mentioned earlier in section 5.4, the no. of mols of any gaseous species depends on the rate of formation of corresponding species and gas flow. In addition, the rate of formation of any species is controlled by the rate of modeled reaction. The modeled reaction with kinetic equation and kinetic parameters are shown in table C3.1:

Table C3.1 Gasification reactions and kinetic parameter

	Reaction	Reaction rate (mol/m^3.s)	A_i (1/s)	E_i (kJ/mol)
R1	Boudouard reaction: $C + CO_2 \leftrightarrow 2CO$	$r_1 = C_{RF} A_1 \exp\left(\frac{-E_1}{RT}\right) \cdot \left(y_{CO_2} - \frac{y_{CO}^2}{K_{eq,1}}\right)$	3.616 x 10^1	77.39
R2	Water-gas reactions: $C + H_2O \leftrightarrow CO + H_2$	$r_2 = C_{RF} A_2 \exp\left(\frac{-E_2}{RT}\right) \cdot \left(y_{H_2O} - \frac{y_{CO} \cdot y_{H_2}}{K_{eq,2}}\right)$	1.517 x 10^4	121.62
R3	Methane formation: $C + 2H_2 \leftrightarrow CH_4$	$r_3 = C_{RF} A_3 \exp\left(\frac{-E_3}{RT}\right) \cdot \left(y_{H_2}^2 - \frac{y_{CH_4}}{K_{eq,3}}\right)$	4.189 x 10^{-3}	19.21
R4	Steam reformation: $CH_4 + H_2O \leftrightarrow CO + 3H_2$	$r_4 = A_4 \exp\left(\frac{-E_4}{RT}\right) \cdot \left(y_{CH_4} \cdot y_{H_2O} - \frac{y_{CO} \cdot y_{H_2}^3}{K_{eq,4}}\right)$	7.301 x 10^{-2}	36.15

The kinetics of char in reduction zone is incorporated via the char reactivity factor (C_{RF}) as the reactivity of char varies along the length of gasifier. The reactions R1, R2 and R3 are multiplied with C_{RF} as these reactions involve the surface reaction with the char present in the reduction zone. Babu & Sheth [27] proposed that the char reactivity vary exponentially along the length of gasification/reduction zone. Thus, the CRF can be estimated along the length of reduction zone as[14];

$$C_{RF} = Ce^{bz} \tag{C3.02}$$

where C = 1, b = 36.7 and z refers to the length of reduction zone (n). In the above mentioned rate reaction expression, $K_{eq,j}$ refers to the equilibrium constant for corresponding reactions and are considered as function of temperature only. $K_{eq,j}$ for each reaction can be calculated by the following mathematical expressions[7]:

$$\ln K_{eq,j} = -\frac{J}{RT} + \Delta A \cdot \ln T + \frac{\Delta B}{2} T + \frac{\Delta C}{6} T^2 + \frac{\Delta D}{2T^2} + I \tag{C3.03}$$

where, J, I, ΔA, ΔB, ΔC and ΔD are thermodynamic constants for particular reaction mechanism. Let's, consider it for methane formation reaction:

Methane formation: $C + 2H_2 \rightarrow CH_4$

then,

$$\Delta A = A_{CH_4} - A_C - 2A_{H_2}$$
$$\Delta B = B_{CH_4} - B_C - 2B_{H_2}$$
$$\Delta C = C_{CH_4} - C_C - 2C_{H_2}$$
$$\Delta D = D_{CH_4} - D_C - 2D_{H_2}$$

The value of A, B, C and D for CH_4 is listed in the thermodynamic property table as in Appendix B1. Then, the values for constants J and I can be estimated as[7]:

$$J = \Delta H_j^0 - R\left(\Delta A \cdot T + \frac{\Delta B}{2}T^2 + \frac{\Delta C}{3}T^3 - \frac{\Delta D}{T}\right) \quad \text{(C3.04)}$$

$$I = \frac{\Delta G_j^0}{RT} - \frac{J}{RT} - \left(\Delta A \cdot \ln T + \frac{\Delta B}{2}T + \frac{\Delta C}{6}T^2 + \frac{\Delta D}{2T^2}\right) \quad \text{(C3.05)}$$

In Eq. (C3.04-05) ΔH_j^0 and ΔG_j^0 are the standard heat of enthalpy and standard Gibbs free energy of the gasification reactions (for instance, methane formation reaction) which is possible to estimate with following equations:

$$\Delta H_{CH_4,298}^0 = h_{CH_4}^0 - h_C^0 - 2h_{H_2}^0 \quad \text{(C3.06)}$$

$$\Delta G_{CH_4,298}^0 = g_{CH_4}^0 - g_C^0 - 2g_{H_2}^0 \quad \text{(C3.07)}$$

The standard heat of formation (h_i^0) and standard Gibbs free energy (g_i^0) for all gaseous species involved in reduction zone are taken from thermodynamic property table B1 from Appendix B. Finally, values of $\Delta G_j^0, \Delta H_j^0$, ΔA, ΔB, ΔC, ΔD, J and I for all reactions (R1-R4) are estimated with similar computational approach and is summarized in Table C3.1.

Table C3.1 Thermodynamic properties for gasification reactions

	$\Delta G°_{298K}$ (kJ/kmol)	$\Delta H°_{298K}$ (kJ/kmol)	ΔA	ΔB	ΔC	ΔD	J (kJ/kmol)	I (kJ/kmol)
R1	120021	172459	-0.476	-7.04E^{-4}	0	1.96E^{+05}	179370.16	25.656
R2	91403	131293	1.384	-1.24E^{-03}	0	7.98E^{+04}	130546.57	7.642
R3	-50460	-74520	-6.567	7.46E^{-03}	-2.16E^{-06}	7.01E^{+04}	-58886.80	32.541
R4	141863	205813	7.951	-8.70E^{-03}	2.16E^{-06}	9.70E^{+03}	189433.31	-24.899

Finally, the values of $K_{eq,j}$ for each reactions are estimated by using parameters as mentioned in Table C3.1 by using Eq. (C3.03).

Similarly, the change in enthalpy (ΔH_{Rj}) of each gasification reaction (R1 to R4) and c_p of each chemical species involved in gasification reaction also plays

significant role in the reaction kinetics in the subsequent Δz compartment and can be calculated as[7];

$$\Delta H^{0}_{R,j} = J + R\left(\Delta A \cdot T + \frac{\Delta B}{2}T^{2} + \frac{\Delta C}{3}T^{3} - \frac{\Delta D}{T}\right) \quad \text{(C3.08)}$$

$$c_p = a + bT + cT^{2} + dT^{3} \quad \text{(C3.09)}$$

The specific heat of gaseous species can be calculated either by correlation as described in Eq. (5.26) or Eq. (C3.09)[49]. The selection of these correlations is basically determined by the model requirement. For instance, Eq. (5.26) has better advantage when change in specific heat is being accounted as it incorporates two temperature limits and had been used to calculate change in enthalpy during energy balance in pyrolysis and oxidation zone. Whereas, Eq. (C3.09) is useful if specific heat at a particular temperature is to be evaluated as in reduction zone.

Once the rate of modeled reaction (r_i) is estimated, the rate of formation of each gaseous species (R_x) involved in gasification reaction is estimated as in table C3.2.

Table C3.2 Net rate of formation of gaseous species by gasification reaction [25]

Species	R_x (mol.m^{-3}.s^{-1})
H_2	r_2-2r_3+3r_4
CO	2r_1+r_2+r_4
CO_2	-r_1
CH_4	r_3-r_4
H_2O	-r_2-r_4
N_2	0

The rate of modeled reaction (r_i) in dependent to temperature and temperature of nth section is determined by modifying Eq. (5.279) and is written as:

$$T_n = T_{n-1} + \left[\frac{1}{v_{n-1}\cdot\sum_x n_i c_{p,i}}\left(-\sum_i r_i \Delta H_i - v_{n-1}\frac{P_n - P_{n-1}}{\Delta z} - P_{n-1}\frac{v_n - v_{n-1}}{\Delta z} - \sum_i R_i c_{p,i} T_{n-1} - Q_R\right)\right]\times \Delta z \quad \text{(C3.10)}$$

Likewise, the gas velocity and pressure at nth section is determined by modifying Eq. (5.29 & 5.30) and is written as:

$$v_n = v_{n-1} + \left[\frac{1}{\sum_i n_i c_{p,i}} \left(\frac{\sum_i n_i c_{p,i} \sum_i R_i}{n} - \frac{\sum_i r_i \Delta H_i}{T_{n-1}} - \frac{P_n - P_{n-1}}{\Delta z} \left(\frac{v_{n-1}}{T_{n-1}} + \frac{v_{n-1} \sum_i n_i c_{p,i}}{P_{n-1}} \right) - \sum_x R_i c_{p,i} \right) \right] \times \Delta z \quad \text{(C3.11)}$$

$$P_n = P_{n-1} + \left[1183 \left(\rho_{gas}^{n-1} \frac{v_{n-1}^2}{\rho_{air}^{n-1}} \right) + 388.19 v_{n-1} - 79.896 \right] \times \Delta z \quad \text{(C3.12)}$$

Furthermore, molar density of air and gas also play important role in kinetic modeling of reduction zone, which can be calculated as;

$$\rho_{air} = \frac{P_n}{R_{specific} \times T_n} \quad \text{where } R_{specific} = 287.058 \text{ Jkg}^{-1}.\text{K}^{-1} \quad \text{(C3.13)}$$

$$\rho_{gas} = \sum_i n_i \times M_i \quad \text{(C3.14)}$$

Finally, the process parameters at n^{th} section (at 0.25 m) is determined by aid of $(n-1)^{th}$ section.

Appendix D VBA code

C1. VBA code executed for the simulation

```
Sub MainMacro()
   Sheets("Pyrolysis").Select
   If Range("B37") = 0 Then
      Call Allok
   Else
     Call Equilibrium
   End If
End Sub
Private Sub Allok()
Msg = "The system is in balance."
Ans = MsgBox(Msg, vbOKCancel)
End Sub

Private Sub Equilibrium()
   Msg = "The system is not in equilibrium, would you like to proceed to mass and
energy balance?"
   Ans = MsgBox(Msg, vbYesNo)
   If Ans = vbYes Then
         Call Balance
         Call Complete
      End If
End Sub

Private Sub Balance()
  Sheets("Pyrolysis").Select
   Range("G19").Select
   Range("G19").GoalSeek Goal:=0, ChangingCell:=Range("C12")
   Range("E19").Select
   Range("E19").GoalSeek Goal:=0, ChangingCell:=Range("E12")
   Range("C19").Select
   Range("C19").GoalSeek Goal:=0, ChangingCell:=Range("B12")
   Range("B37").Select
   Range("B37").GoalSeek Goal:=0, ChangingCell:=Range("E23")
   Sheets("Oxidation").Select
   Range("G54").Select
   Range("G54").GoalSeek Goal:=0, ChangingCell:=Range("C35")
   Range("C54").Select
   Range("C54").GoalSeek Goal:=0, ChangingCell:=Range("B35")
   If Range("B35") > 0 Then
      Range("B35") = Range("B35")
      Range("C39") = 0
      Range("D39") = 0
      Range("B40") = 0
      Range("E40") = 0
```

```
        Range("C40") = 0
        Range("F40") = 0
    Else
        Range("B35") = 0
        Range("C54").Select
        Range("C54").GoalSeek Goal:=0, ChangingCell:=Range("C35")
        If Range("D36") - Range("G54") < 0 Then
            Range("D39") = Range("D36")
            Range("C39") = Range("D39")
        Else
            Range("D39") = Range("G54")
            Range("C39") = Range("D39")
        End If
        If Range("B40") > 0 Then
          Range("E40") = Range("B40") / 2
          Range("C40") = Range("B40") / 2
          Range("F40") = Range("B40")
        Else
          Range("E40") = 0
          Range("C40") = 0
          Range("F40") = 0
        End If
    End If
    Range("B65").Select
    Range("B65").GoalSeek Goal:=0, ChangingCell:=Range("E28")
    Sheets("Results").Select
End Sub

Private Sub Complete()
Msg = "The system is now in equilibrium."
Ans = MsgBox(Msg, vbOKCancel)
End Sub
```

. . . . . .

12 References

[1] P. Basu, "Chapter 5 - gasification theory and modeling of gasifiers," in *Biomass Gasification and Pyrolysis*Anonymous Boston: Academic Press, 2010, pp. 117-165.

[2] A. Rajvanshi, "Biomass gasification," in *Alternative Energy in Agriculture*, 2nd ed., Y. Goswami, Ed. U.S.A: CRC Press, 1986, pp. 83-103.

[3] M. Puig-Arnavat, J. C. Bruno and A. Coronas, "Review and analysis of biomass gasification models," *Renewable and Sustainable Energy Reviews,* vol. 14, pp. 2841-2851, 12, 2010.

[4] N. Gao and A. Li, "Modeling and simulation of combined pyrolysis and reduction zone for a downdraft biomass gasifier," *Energy Conversion and Management,* vol. 49, pp. 3483-3490, 12, 2008.

[5] A. Melgar, J. F. Pérez, H. Laget and A. Horillo, "Thermochemical equilibrium modelling of a gasifying process," *Energy Conversion and Management,* vol. 48, pp. 59-67, 1, 2007.

[6] S. Jarungthammachote and A. Dutta, "Thermodynamic equilibrium model and second law analysis of a downdraft waste gasifier," *Energy,* vol. 32, pp. 1660-1669, 9, 2007.

[7] Z. A. Zainal, R. Ali, C. H. Lean and K. N. Seetharamu, "Prediction of performance of a downdraft gasifier using equilibrium modeling for different biomass materials," *Energy Conversion and Management,* vol. 42, pp. 1499-1515, 8, 2001.

[8] X. Li, J. R. Grace, A. P. Watkinson, C. J. Lim and A. Ergüdenler, "Equilibrium modeling of gasification: a free energy minimization approach and its application to a circulating fluidized bed coal gasifier," *Fuel,* vol. 80, pp. 195-207, 1, 2001.

[9] M. J. Prins, K. J. Ptasinski and F. J. J. G. Janssen, "From coal to biomass gasification: Comparison of thermodynamic efficiency," *Energy,* vol. 32, pp. 1248-1259, 7, 2007.

[10] R. H. Perry and D. W. Green, *Perry's Chemical Engineers' Handbook*. McGraw Hill, 1997.

[11] C. Koroneous and S. Lykidou, "Equilibrium modeling for a downdraft biomass gasifier for cotton stalks biomass in comparision with experimental data," *Journal of Chemical Engineering and Materials Science,* vol. 2, pp. 61-68, 2011.

[12] J. K. Ratnadhariya and S. A. Channiwala, "Three zone equilibrium and kinetic free modeling of biomass gasifier – a novel approach," *Renewable Energy,* vol. 34, pp. 1050-1058, 4, 2009.

[13] A. V. Bridgwater, "Review of fast pyrolysis of biomass and product upgrading," *Biomass Bioenergy,* vol. 38, pp. 68-94, 3, 2012.

[14] F. Centeno, K. Mahkamov, E. E. Silva Lora and R. V. Andrade, "Theoretical and experimental investigations of a downdraft biomass gasifier-spark ignition engine power system," *Renewable Energy,* vol. 37, pp. 97-108, 1, 2012.

[15] P. Koukkari and R. Pajarre, "Introducing mechanistic kinetics to the Lagrangian Gibbs energy calculation," *Comput. Chem. Eng.,* vol. 30, pp. 1189-1196, 5/15, 2006.

[16] I. Antonopoulos, A. Karagiannidis, A. Gkouletsos and G. Perkoulidis, "Modelling of a downdraft gasifier fed by agricultural residues," *Waste Manage.,* vol. 32, pp. 710-718, 4, 2012.

[17] S. Jarungthammachote and A. Dutta, "Equilibrium modeling of gasification: Gibbs free energy minimization approach and its application to spouted bed and spout-fluid bed gasifiers," *Energy Conversion and Management,* vol. 49, pp. 1345-1356, 6, 2008.

[18] A. K. Sharma, "Equilibrium and kinetic modeling of char reduction reactions in a downdraft biomass gasifier: A comparison," *Solar Energy,* vol. 82, pp. 918-928, 10, 2008.

[19] G. Várhegyi, M. J. Antal Jr., E. Jakab and P. Szabó, "Kinetic modeling of biomass pyrolysis," *J. Anal. Appl. Pyrolysis,* vol. 42, pp. 73-87, 6, 1997.

[20] P. Basu, "Chapter 3 - pyrolysis and torrefaction," in *Biomass Gasification and Pyrolysis*Anonymous Boston: Academic Press, 2010, pp. 65-96.

[21] A. F. Roberts, "A review of kinetics data for the pyrolysis of wood and related substances," *Combust. Flame,* vol. 14, pp. 261-272, 4, 1970.

[22] A. K. Sharma, "Modeling and simulation of a downdraft biomass gasifier 1. Model development and validation," *Energy Conversion and Management,* vol. 52, pp. 1386-1396, 2, 2011.

[23] A. K. Sharma, M. R. Ravi and S. Kohli, "Modeling product composition in slow pyrolysis of wood," *Mechanical Engineering Department, Indian Institute of Technology, Delhi-110016,* vol. 16, pp. 1-11, SESI J, 2006.

[24] S. Sommariva, R. Grana, T. Maffei, S. Pierucci and E. Ranzi, "A kinetic approach to the mathematical model of fixed bed gasifiers," *Comput. Chem. Eng.,* vol. 35, pp. 928-935, 5/11, 2011.

[25] D. L. Giltrap, R. McKibbin and G. R. G. Barnes, "A steady state model of gas-char reactions in a downdraft biomass gasifier," *Solar Energy,* vol. 74, pp. 85-91, 1, 2003.

[26] Y. Wang and C. M. Kinoshita, "Kinetic model of biomass gasification," *Solar Energy,* vol. 51, pp. 19-25, 7, 1993.

[27] B. V. Babu and P. N. Sheth, "Modeling and simulation of reduction zone of downdraft biomass gasifier: Effect of char reactivity factor," *Energy Conversion and Management,* vol. 47, pp. 2602-2611, 9, 2006.

[28] P. C. Roy, A. Datta and N. Chakraborty, "Modelling of a downdraft biomass gasifier with finite rate kinetics in the reduction zone," *Int. J. Energy Res.,* vol. 33, pp. 833-851, 2009.

[29] P. Pepiot, C. J. Dibble and T. D. Foust, "Computational fluid dynamics modeling of biomass gasification and pyrolysis," in Anonymous American Chemical Society, 2010, pp. 273-298.

[30] I. Janajreh and M. Al Shrah, "Numerical and experimental investigation of downdraft gasification of wood chips," *Energy Conversion and Management,* vol. 65, pp. 783-792, 1, 2013.

[31] D. F. Fletcher, B. S. Haynes, F. C. Christo and S. D. Joseph, "A CFD based combustion model of an entrained flow biomass gasifier," *Appl. Math. Model.,* vol. 24, pp. 165-182, 3, 2000.

[32] L. Yu, J. Lu, X. Zhang and S. Zhang, "Numerical simulation of the bubbling fluidized bed coal gasification by the kinetic theory of granular flow (KTGF)," *Fuel,* vol. 86, pp. 722-734, 0, 2007.

[33] d. S. MaurÃcio Bezerra Jr, C. N. Leonardo, G. B. Amaro Jr and P. B. Cristina, "Neural network based modeling and operational optimization of biomass gasification processes," in Anonymous 2012, .

[34] T. H. Jayah, L. Aye, R. J. Fuller and D. F. Stewart, "Computer simulation of a downdraft wood gasifier for tea drying," *Biomass Bioenergy,* vol. 25, pp. 459-469, 10, 2003.

[35] M. Barrio and M. Fossum, "Operational characteristics of a small-scale stratified downdraft gasifier," in *Technologies and Combustion for a Clean Environment Sixth International Conference,* 2001.

[36] R. Shand and A. Bridgewater, "Fuel gas from biomass: Status and new modeling approaches," in *Thermochemical Processing of Biomass*, A. V. Bridgwater, Ed. London: Butterworths, 1984, pp. 229-254.

[37] S. A. Channiwala and P. P. Parikh, "A unified correlation for estimating HHV of solid, liquid and gaseous fuels," *Fuel,* vol. 81, pp. 1051-1063, 5, 2002.

[38] D. A. Tillman, A. J. Rossi and W. D. Kitto, "Chapter 2-properties of wood fuels," in *Wood Combustion*Anonymous Academic Press, 1981, pp. 17-47.

[39] H. Thunman, F. Niklasson, F. Johnsson and B. Leckner, "Composition of Volatile Gases and Thermochemical Properties of Wood for Modeling of Fixed or Fluidized Beds," *Energy Fuels,* vol. 15, pp. 1488-1497, 11/01; 2013/01, 2001.

[40] K. W. Ragland, D. J. Aerts and A. J. Baker, "Properties of wood for combustion analysis," *Bioresour. Technol.,* vol. 37, pp. 161-168, 1991.

[41] A. TenWolde, J. D. McNatt and L. Krahn, "Thermal properties of wood and wood panel products for use in buildings." *DOE/USDA-21697/1.*

[42] S. R. Turn, "Chapter 2 - combustion and thermochemictry," in *An Introduction to Combustion*, 2nd ed.Anonymous Boston: McGraw Hill, 2000.

[43] C. Storm, H. RuÌˆdiger, H. Spliethoff and K. R. G. Hein, "Co-Pyrolysis of Coal/Biomass and Coal/Sewage Sludge Mixtures," *Journal of Engineering for Gas Turbines and Power,* vol. 121, pp. 55-63, 01/01, 1999.

[44] B. Srinivas and N. R. Amundson, "A single-particle char gasification model," *AIChE J.,* vol. 26, pp. 487-496, 1980.

[45] M. W. Thring, *The Science of Flames and Furnaces.* London: Chapman & Hall, 1952.

[46] P. Basu, "Chapter 6 - design of biomass gasifiers," in *Biomass Gasification and Pyrolysis*Anonymous Boston: Academic Press, 2010, pp. 167-228.

[47] J. T. Konttinen, A. Moilanen, N. DeMartini and M. Hupa, "Carbon conversion predictor for fluidized bed gasification of biomass fuelsâ€"from TGA measurements to char gasification particle model," *Biomass Conversion and Biorefinery,* vol. 2, pp. 265-274, 09/01, 2012.

[48] Z. A. Zainal, A. Rifau, G. A. Quadir and K. N. Seetharamu, "Experimental investigation of a downdraft biomass gasifier," *Biomass Bioenergy,* vol. 23, pp. 283-289, 10, 2002.

[49] Y. A. Cengel and M. A. Boles, *Thermodynamics: An Engineering Approach.* McGraw Hill, 2006.

[50] P. Basu, "Appendix C - selected design data tables," in *Biomass Gasification and Pyrolysis*Anonymous Boston: Academic Press, 2010, pp. 329-335.

[51] F. V. Tinaut, A. Melgar, J. F. Pérez and A. Horrillo, "Effect of biomass particle size and air superficial velocity on the gasification process in a downdraft fixed bed gasifier. An experimental and modelling study," *Fuel Process Technol,* vol. 89, pp. 1076-1089, 11, 2008.